



Highly Conductive Custom Inks for Aerospace Applications

**James Mason
Xactiv Inc.**

**06/26/2020
Final Report**

DISTRIBUTION A: Distribution approved for public release.

**Air Force Research Laboratory
AF Office Of Scientific Research (AFOSR)/ RTA1
Arlington, Virginia 22203
Air Force Materiel Command**

DISTRIBUTION A: Distribution approved for public release

REPORT DOCUMENTATION PAGE			<i>Form Approved</i> <i>OMB No. 0704-0188</i>		
<p>The public reporting burden for this collection of information is estimated to average 1 hour per response, including the time for reviewing instructions, searching existing data sources, gathering and maintaining the data needed, and completing and reviewing the collection of information. Send comments regarding this burden estimate or any other aspect of this collection of information, including suggestions for reducing the burden, to Department of Defense, Executive Services, Directorate (0704-0188). Respondents should be aware that notwithstanding any other provision of law, no person shall be subject to any penalty for failing to comply with a collection of information if it does not display a currently valid OMB control number.</p> <p>PLEASE DO NOT RETURN YOUR FORM TO THE ABOVE ORGANIZATION.</p>					
1. REPORT DATE (DD-MM-YYYY) 05-07-2020		2. REPORT TYPE Final Performance		3. DATES COVERED (From - To) 01 Apr 2019 to 31 Mar 2020	
4. TITLE AND SUBTITLE Highly Conductive Custom Inks for Aerospace Applications			5a. CONTRACT NUMBER		
			5b. GRANT NUMBER FA9550-19-1-0143		
			5c. PROGRAM ELEMENT NUMBER 61102F		
6. AUTHOR(S) James Mason			5d. PROJECT NUMBER		
			5e. TASK NUMBER		
			5f. WORK UNIT NUMBER		
7. PERFORMING ORGANIZATION NAME(S) AND ADDRESS(ES) Xactiv Inc. 71 Perinton Pkwy Fairport, NY 14450-9104 US			8. PERFORMING ORGANIZATION REPORT NUMBER		
9. SPONSORING/MONITORING AGENCY NAME(S) AND ADDRESS(ES) AF Office of Scientific Research 875 N. Randolph St. Room 3112 Arlington, VA 22203			10. SPONSOR/MONITOR'S ACRONYM(S) AFRL/AFOSR RTA1		
			11. SPONSOR/MONITOR'S REPORT NUMBER(S) AFRL-AFOSR-VA-TR-2020-0030		
12. DISTRIBUTION/AVAILABILITY STATEMENT A DISTRIBUTION UNLIMITED: PB Public Release					
13. SUPPLEMENTARY NOTES					
14. ABSTRACT There were four objectives to the research undertaken: improvement of carbon based resistive inks suitable for inkjet deposition, development of carbon based resistive inks that have low (less than 150C) cure temperature, development of silver nanomaterial ink for transparent conductive coatings, and exploration of inkjettable materials for semiconductor devices. The first objective achieved a cost effective all carbon ink capable of ~100 ohm/square in a single inkjetted layer and ~30 ohm/square (7.83E-03 ohm-cm volume resistivity) with three layers with reliable jetting and kilogram scale production capacity. Development of low cure temperature carbon inks was rendered unnecessary by the successful development of an alternative cure process using low temperature drying followed by UV flashlamp curing. Silver nanomaterial and silver complex inks were manufactured in Xactiv's lab and achieved ~80% transparency with single digit ohm/square conductivity, but did not exhibit performance improvement over commercially available nanomaterials. The effort to explore inkjettable materials for semiconductors revealed more materials development work is needed before inkjettable semiconductors can be produced in commercial quantity, non-lab environments.					
15. SUBJECT TERMS ink, conductive, ink jet, dispersion, polymer, powder, semiconductor					
16. SECURITY CLASSIFICATION OF:			17. LIMITATION OF ABSTRACT UU	18. NUMBER OF PAGES	19a. NAME OF RESPONSIBLE PERSON GORETTA, KENNETH
a. REPORT Unclassified	b. ABSTRACT Unclassified	c. THIS PAGE Unclassified			

Standard Form 298 (Rev. 8/98)
Prescribed by ANSI Std. Z39.18

DISTRIBUTION A: Distribution approved for public release

				19b. TELEPHONE NUMBER <i>(Include area code)</i> 703-696-7349
--	--	--	--	---

Final Performance Report



Air Force Grant Award FA9550-19-1-0143

Highly Conductive Inks for Aerospace Applications

Contributors:

James Mason

Leonard Carreira

Rachel Collier

Carl Felice

Louis Isganitis

Samantha Lauro

Peter Mason

Leonard Shellhammer

Special Thanks to:

Dr. Ken Goretta, Program Officer AFOSR

1.0 Summary

This report describes work done at XACTIV under Air Force Grant Award FA9550-19-1-0143. The report covers work on four projects undertaken over the grant period. The projects are listed below:

1. Development and scale up of carbon inks to achieve high conductivity.
2. Development of conductive carbon inkjet inks that can be cured at temperatures of 150 °C or less for use on various flexible substrates.
3. Development of a transparent, conductive silver ink.
4. Exploration of materials and methods to create inkjet inks for construction of printable semiconductor and electronic devices.

2.0 Project 1: High conductivity carbon inkjet inks

2.1 Introduction

For years XACTIV has been engaged in a program of developing carbon-based inks of increasingly higher conductivity. A key requirement has been for these inks to be used in commercially available ink jet printheads, allowing the printing of products with variable content. This requirement also places limits on the composition of the ink as it relates to properties such as viscosity and surface tension, which must be controlled within certain ranges to ensure printhead operability. The inks are aqueous dispersions of various forms of conductive carbon particles. Cosolvents must be chosen to prevent the ink drying out too quickly in the nozzles of the printhead. Another key requirement is that the resulting ink formulation be stable and not have the solids irreversibly agglomerate and settle in a short period of time.

This report describes two efforts undertaken to address the goal of achieving higher conductivity inks based on carbon pigments:

The first objective was the scale up of a recently completed ink design at XACTIV, known as Type 6 ink. The scale up required development of a new process within XACTIV for processing carbon pigment-based inks. The report describes the production and characterization of an approximately six gallon batch of ink that, when printed, demonstrated a sheet resistance of under 100 ohms/square.

The second objective was the design of a next generation conductive carbon ink with the goal of achieving a sheet resistance of less than 10 ohms/square. Essential to this task was the equipment and process experience used in the scale up done in the previous task. An ink formulation and process from this work resulted in printing with a measured sheet resistance of 18 ohms/square in three passes at 50% area coverage per pass.

2.2 Objective 1: Scale up of Type 6 Ink

2.2.1 Background

At the end of 2018, an XACTIV internal report documented the work that led to a new carbon ink, Type 6, with a lower resistivity than the previous benchmark, which was Type 5. Although all these inks are water-based, Type 6 ink has a different solvent system than Type 5. Ink cosolvents are typically chosen to have a lower vapor pressure than water, to slow ink drying out in the printhead. In the case of Type 6, in addition to lower vapor pressure than water, the cosolvents were also selected for their viscosity, with lower viscosity being preferable. Previous ink design work showed that to maximize printed conductivity with the least amount of deposited material, it is desirable to load the ink with as high a weight per cent as possible of the conducting pigments. But one limit for pigment loading is ink viscosity which, if it gets too high, will render the ink inoperable in the printhead. The solvents chosen also promote penetration of the ink into certain printed substrates. At high printed ink densities, previous ink designs pooled on the surface, even when the same ink deposition was spread out over multiple passes. This pooling leads to mottling and nonuniformity of the surface and ultimately lowers the conductivity and precision relative to a uniform distribution of the conductive solids.

2.2.2 Scale up equipment and process details

The ink design was developed using a new process compared to previous designs. The newest form of carbon pigment, henceforth called carbon₁, needed to be reduced in size and this was initially accomplished by roll milling the dispersion in glass jars with steel balls for extended periods of time. Key to the development of a scaled-up Type 6 process was the acquisition of a Union Process SD-1 attritor at the beginning of 2019. The unit acquired had a polymer lined grinding flask. It also came with an accessory kit that enabled the use of a small, 750 ml grind flask for processing smaller batches. Both a polymer lined and stainless-steel version of the 750 ml flask were acquired. To run the smaller grind flask, a cover was supplied that went over the opening of the main grinding flask (see Figure 1). Four clamps held the top in place as shown in the figure. Cooling fluid lines for incoming and outgoing cooling fluid are shown toward the back. An in-house chiller system set to 4 °C provided chilling fluid to the unit. When using a large 1.5-gallon grind flask, cooling fluid is sent to the jacket of the flask. When the 750 ml flask is used, the cooling fluid circulates inside the gallon sized grinding flask in which the smaller flask sits. Batch temperature during grinding is typically on the order of 10°C. The cover accessory used to enable use of the small flask was sealed to the larger grinding flask via an O-ring at the edge of the cover. An O-ring around the center opening of the cover was used to seal the lip of the small flask to the cover, with sealing pressure applied by clamps screwed into three holes space symmetrically around the center opening. Two of those screw holes are visible in Figure 1.



Figure 1: Top of 1.5-gallon grinding flask with cover for 750 ml flask use.

From early batches made with the small flask using various grinding media, including ceramic and tungsten carbide media, it very quickly became apparent that stainless steel media (1/8" 440C stainless-steel balls) was the best to use to achieve the desired size reduction most efficiently. To do larger batches, a 1.5-gallon stainless steel lined grinding flask along with stainless steel rotor arm and shaft were acquired, since the polymer lined flask and associated shaft and arms were not usable with the chosen media. The Type 6 scaled up process was developed using this new grinding flask, shaft, and arms. The new flask was modified to accommodate the cover accessory that enabled use of the smaller, 750 ml grind flask. The polished stainless-steel lined smaller flask was used to develop the next generation carbon ink design.

The Type 6 ink formulation consists of several forms of carbon and, a number of liquids in which the carbons are dispersed, the primary one being water. There are also some minor ingredients in the categories of dispersants, surfactants, binders, pH adjustors, etc. Experience with previous carbon ink designs led to the conclusion that it was not necessary for further size reduction of some forms of carbon utilized in the design than that achieved with earlier processes. However, the carbon1 pigment in the Type 6 design did require grinding. Therefore, a process was developed whereby an initial mill base was prepared containing only carbon1 and other, non-pigment ink ingredients. After that was milled, the other forms of carbon were slowly added to the attritor and the milling continued for a much shorter time.

A further refinement to the process was made when it was observed that milling carbon1 with the remainder of the ink ingredients except the other carbons led to a mill base with relatively low viscosity. The low viscosity limited the speed at which the attritor could be run due to mill base sloshing out the top of the attritor flask. The final process mills carbon1 at twice its normal concentration in the ink, which leads to a higher viscosity mill base that can be run at higher speeds, without losing material out the top.

A further improvement made was to use the accessory cover on the attritor that is normally used to hold the smaller, 750 ml flask when running a batch in the 1.5-gallon grind tank. The use of the cover prevents sloshing of the mill base out of the attritor and thus enables higher attritor speeds to be run, resulting in minimization of milling times. As shown in Figure 1, a plastic coffee pot lid had a hole cut in its center to enable the attritor rotor shaft to pass. This formed a perfectly sized cover for this configuration.

The first time the new stainless steel lined grinding flask was used, a new 7.5" diameter shaft with arms was installed and spaced 3/8" (3X the media diameter) away from the bottom of the of the flask as specified by the manufacturer. 40 pounds of 1/8" stainless steel ball media were put into the grinding flask and the flask filled with 3 liters of water. The attritor was run at 1200 RPM motor speed for 10 minutes. The water was changed four times and the attritor was refilled with water containing Alconox cleaner and run for ½ hour. The water was drained and the flask flushed with clean water 3-4 times and refilled with DI water. The attritor was run for an hour, flushed, and filled with clean DI water for a final rinse.

See Table 1 for information on attritor speed settings. As noted above, 40 pounds was the usual charge of media for the large grind flask. When running at this scale the speed settings used evolved, changing to higher speeds when the process was modified to mill the carbon1 by itself in a higher viscosity mill base. 800g of this media was the standard charge for the 750 ml flask. The attritor was usually set to 1800 RPM for runs at this scale, giving a tip speed of 392 feet/minute for the 2.5" diameter arms.

During attritor runs, samples were taken periodically for particle size measurement as well as sheet resistance of a draw down sample. The attrition step was usually followed by another process step to promote the dispersion of the pigments. All inks were also

filtered before ink jet printing. Small amounts were filtered through a 1 micron, 37 mm wide glass fiber filter (Pall #4524). Larger amounts were filtered through a 5 or 10-micron Meisner capsule filter.

Table 1: Attritor Speed Converter

<u>Large Pot</u>			
Rotor Constant	Motor RPM	Rotor RPM	Feet/Min
1.9635	1800	599.4	1176.9
1.9635	1700	566.1	1111.5
1.9635	1600	532.8	1046.2
1.9635	1500	499.5	980.8
1.9635	1400	466.2	915.4
1.9635	1300	432.9	850.0
1.9635	1200	399.6	784.6
1.9635	1100	366.3	719.2
1.9635	1000	333	653.8
1.9635	900	299.7	588.5
1.9635	800	266.4	523.1
1.9635	700	233.1	457.7
1.9635	600	199.8	392.3
1.9635	500	166.5	326.9
1.9635	400	133.2	261.5
1.9635	300	99.9	196.2
1.9635	200	66.6	130.8
1.9635	100	33.3	65.4
1.9635	50	16.65	32.7
<u>Small Pot</u>			
Rotor Constant	Motor RPM	Rotor RPM	Feet/Min
0.6545	1800	599.4	392.3
0.6545	1700	566.1	370.5
0.6545	1600	532.8	348.7
0.6545	1500	499.5	326.9
0.6545	1400	466.2	305.1

Inks were screened for sheet resistance using a draw down, usually with a #5 wire wound bar obtained from R.D. Specialties, Webster, NY. The draw down was usually done on a glass-fabric, bias weave reinforced honeycomb (HexWeb® HRH-327 from Hexcel), hereafter in this report called polyglass. The sample was dried and cured in an oven before measurement. Sheet resistance was measured using a 4-point probe (RCHEK

model RC 2175 from EDTM). Particle size measurements were made on a Malvern 2000S. Ink jetting performance was characterized in fixture utilizing a Dimatix Galaxy 80 pl printhead.

Layer thickness of dried drawdowns was calculated using the draw down wet thickness and the volume fraction of each of the ingredients calculated using the ink formulation and the density of each component. The volume fraction of the nonvolatile ingredients was used as an estimate the thickness of the dried layer.

Where noted, ink viscosity was measured using an Atago portable viscometer with the low viscosity attachment. Surface tension was measured with a Krüss Model K-20 tensiometer.

2.2.3 First Scale Up: Ink 19126S

Initial experiments using the 750 ml grinding flask led to the conclusion that 1/8" stainless steel balls were the right media to use. Batch 19112 started on April 22, 2019 was the prototype recipe used for scaling up to the large grinding flask. The recipe was scaled up by a factor of 7.5. For this first scale up run with the new large stainless-steel grinding flask and media, the following process steps were used:

- 1) Prepare attritor for dispersion (clean and rinse)
- 2) Prepare carbon1 dispersion for milling
- 3) Add dispersion to attritor flask
- 4) Run attritor for specified time period
- 5) Add other mixed carbon powders
- 6) Run attritor for additional (short) time specified
- 7) Remove ink from attritor
- 8) Process in an additional dispersion step
- 9) Filter ink

After the attritor was cleaned and the ingredients mixed, the attritor was turned on and the cooling water circulated in the jacket around the grinding flask. The initial motor speed was 198 RPM which corresponds to 60 RPM for the attritor rotor speed. The composition 19126S was slowly added to the attritor flask. When all the material was in the flask, the attritor motor speed was increased to 600 RPM. At this motor speed the rotator tip speed matches the 392 fpm tip speed of the small 750cc flask. See Table 1 for speed comparisons. At this speed, the ink level was nearly to the top of the flask. Attempts to increase the tip speed to 450 fpm (~700 RPM) caused the ink to wet the lid area of the flask.

The literature from Union Process claimed the large flask should run at a tip speed of 600-1000 fpm. The plan was to operate at the higher tip speeds in the larger grind flask under the assumption that this would mean shorter run times to achieve the desired size reduction. But because of this ink level problem limiting the rotor speed, for this run the

processing time had to match the 48-hour grind time achieved with the 750 ml grinding flask.

The initial fluid containing only carbon¹ was milled for a total 50 hours. The attritor speed was reduced to 198 RPM and the other carbon powders were slowly added to the mixture in the flask. The attritor speed was slowly increased to the previous operating speed in order to wet the powders. At that point it was observed that the increase in ink viscosity caused by the addition of the carbon powders lowered the swirling ink level in the flask. The attritor speed could be increased to 1000 RPM to match the swirling level observed with the initial ink. This is a tip speed of about 654 fpm or a 67% increase. This result suggested that increasing the viscosity of the initial carbon mix might be a way to get a better milling condition for the first milling stage.

The ink was milled for 1½ hour at the higher speed and then the speed was reduced to 198 RPM as the ink was drained into a stainless-steel flask using the attritor's bottom drain valve. The ink was then run through the additional dispersion step.

The ink was then filtered through a 5µ Meisner capsule filter. The system pressure increased rapidly so that only 502g of ink was filtered through one filter. The D90 for the ink shown in Table 2 is 2.3µ. It is possible there was a sufficient number of large particles to clog the filter but the result was considered unusual for the filter to clog with so little ink. After the ink was filtered the D90 value dropped to 0.712µ.

Ink was sampled throughout the ink processing for particle size distribution and surface resistance measurements at intervals shown in the last column of Table 2. The maximum ink sample removed was 7g (77g maximum for the entire run). The ink viscosity was measured after the ink was removed from the attritor. The ink viscosity was 24 centipoise at 9°C ink temperature. The process temperature of the ink in the flask stayed between 8°C and 10°C throughout the milling.

The change in surface resistance with milling time, running the dispersing step, and then filtering is shown in Figure 2. The blue curve shows the typical power curve reduction of resistance with milling time. The red data point at 51 hours is the change in resistance after addition of the other carbons and 2 minutes of mixing. The red data point at 52 hours is the change after 1.5 hours of additional milling. The last three red data points are after 12 hours of refrigeration, processing through a dispersion step, and final filtration through the 5µ Meisner filter. Each of the following four graphs, Figures 2 to 4, will have the same five red data points just referenced.

In Figure 3, the D50 value plotted against increasing milling time shows a trend like that of the surface resistance. In the case of D50 there is a more consistent reduction in particle size as additional work is done on the ink by the additional dispersion step and filtration. The D10 plot shown in Figure 4 also shows a similar trend to surface resistance and D50.

Table 2: Properties of Ink 19126S

Mix/Ink	Particle Size Distribution (nm)				R _s	Sample Description
Attritor #/Ink	SSA (m ² /g)	D10	D50	D90	Ω/□	Details
19126S	0.83	6.72	28.338	134.72		1 minute milling
19126S	9.06	0.224	3.818	25.651	623	1 hr milling
19126S	13.6	0.138	1.785	32.106	522	3 hr milling
19126S	14.9	0.125	1.490	32.926	401	5 hr milling
19126S	23.5	0.089	0.961	23.837	250	21.5 hr milling
19126S	23.5	0.088	1.039	26.44	231	24 hr milling
19126S	35.7	0.074	0.207	9.563	166	50 hr milling
19126S-C2M	30.7	0.079	0.315	11.813	128	Carbons added /2 minute milling
19126S-C1HR	35.7	0.074	0.207	9.563	135	1.5 hr milling
19126S-50R	31.9	0.077	0.263	13.27	114	Overnight refrigerate
19126S-D	58.0	0.05	0.123	2.283	152	Dispersion Step
19126S-D5F	62.8	0.053	0.098	0.712	188	5 micron filtration/502g

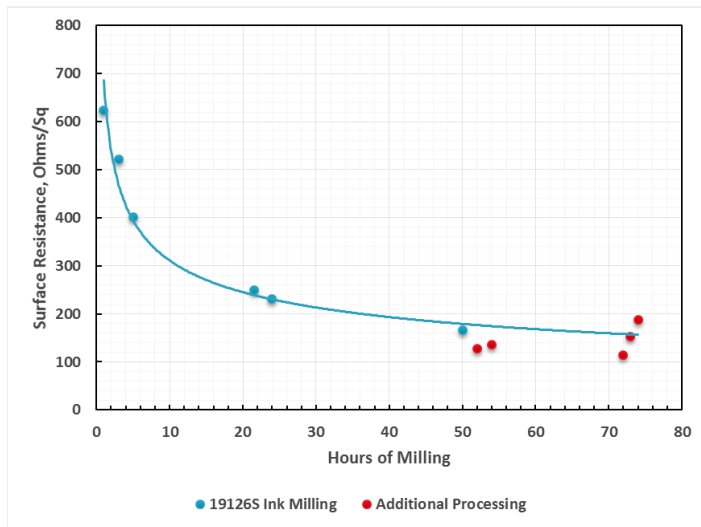


Figure 2: Surface Resistance vs. Milling Time of 19126S

The last PSD parameter describing the size distribution is D90, plotted in Figure 5. This value does not follow the same size reduction trend as the D50 and D10. It is missing the rapid size reduction during the initial 10 hours of milling. The first 24 hours of milling make very little impact on the upper end of the size distribution. Improved milling of the high end of the distribution would reduce the milling time of the ink significantly.

The last measured parameter is the specific surface area of the ink that correlates inversely to the decrease in particle diameter of the distribution. This parameter is plotted

in Figure 6. The red data points demonstrate the dramatic increase in area after the additional dispersion step and filtering of the ink. It suggests that the additional dispersion step increases the probability that the larger aggregates are broken up as compared to the attritor's more random collisions.

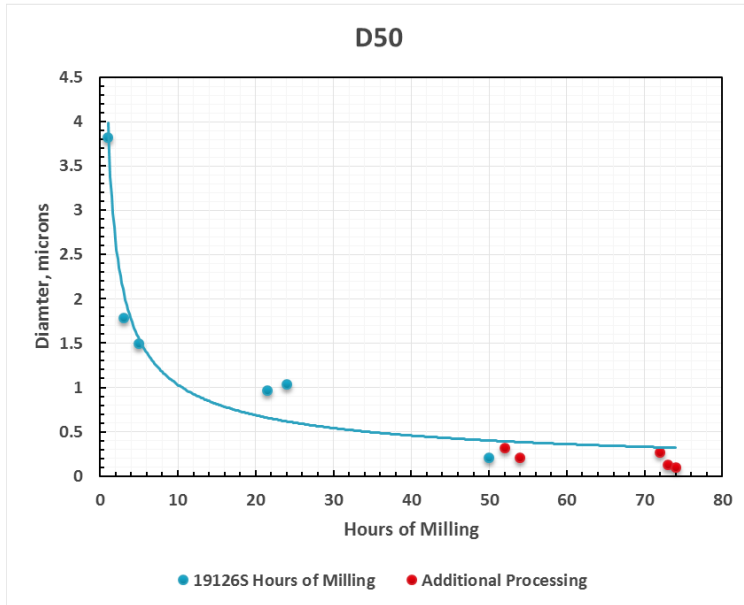


Figure 3: D50 vs. Milling Time of 19126S

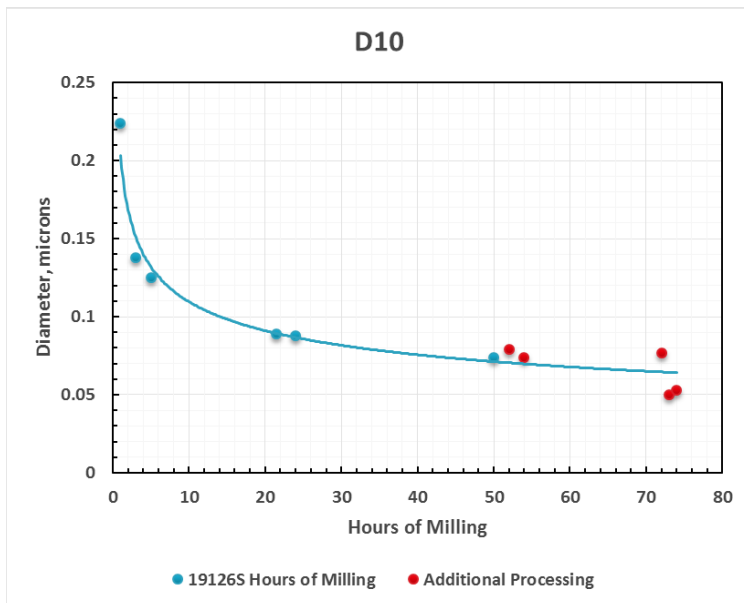


Figure 4: D10 vs. Milling Time of 19126S

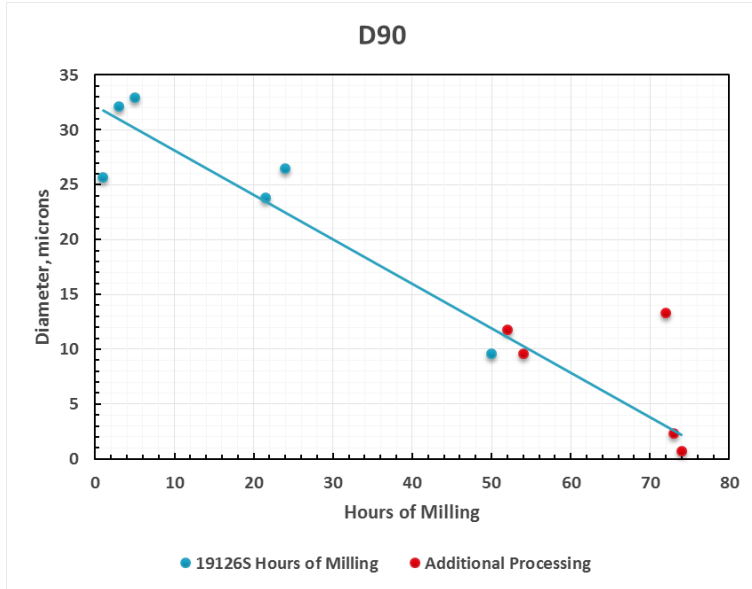


Figure 5: D90 vs. Milling Time of 19126S

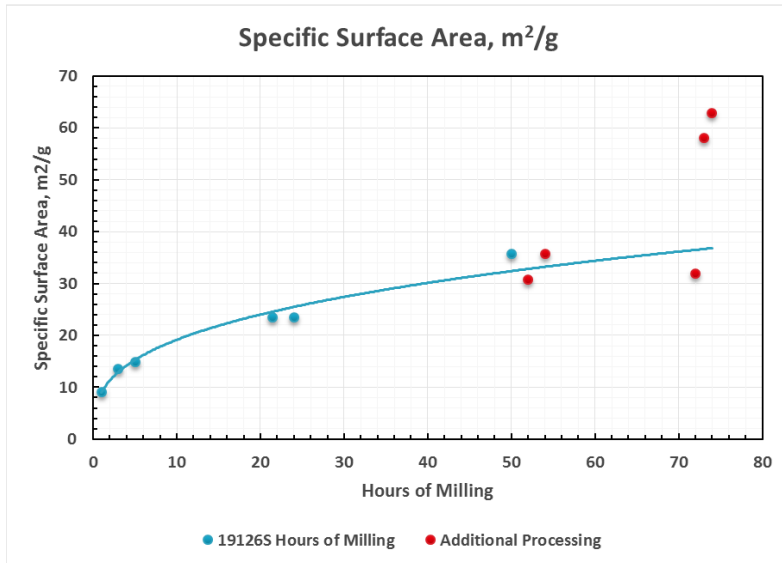


Figure 6: Specific Surface Area vs. Milling Time of 19126S

The process yield was measured because of a concern about the amount of ink that is entrained in the 40 pounds of 1/8 inch steel shot. Table 3 shows the initial ink mass and the mass collected after the attritor processing and the additional dispersion step. The yield after each process step was about 95%. The loss after attrition was not as great as expected and was better than that of the additional dispersion step. The filtering step had losses due to leaks along with the pressure build up that required filter changes, so data on filtration is not shown. Extrapolating from these results point to a final yield in the range of 80-85%.

The physical properties of the final filtered ink can be seen in Table 4. The ink was filtered on May 9th and refrigerated until the physical properties were measured on May 17th. This was after about one week at 8°C in the lab refrigerator.

Table 3: Process Yield

Process Step	Mass, g	% Yield	Cumulative % Yield
Initial	3165		
Attritor	3059	96.65 ^a	
Dispersion	2870	93.84 ^b	90.68
Filtration			
^a Includes 63 g removed for testing.			
^b Includes 14 g removed for testing.			

Table 4: Properties of Ink 19126S

Time	Viscosity	Surface Tension	Ink Mass	SSA	Partical Size Distribution, μ			Sur. Res.
Weeks	cPs	mN/m	%	m ² /g	D10	D50	D90	Ω/\square
0	14.36	43.8	14.4	59.6	0.05	0.118	1.268	188
1	47.89	43.5		50.1		0.226	1.797	

The surface resistance appears a little higher than expected and might be the result of insufficient milling of carbon1. The total ink solids appear low based on the formulation. The total ink solids after heating to the cured state should be 13.57% for phase 1 (milling of carbon1) and 18.16% after the ink is completed. Measurements made during processing averaged 12.74% and 17.44% respectively. The differences can be a result of the curing time and temperature being very different.

As shown in Table 4, properties of the ink were re-measured one week after the first measurements. There is a major increase in ink viscosity and a shift to larger particles resulting in lower specific surface area and increasing D50 and D90 particle sizes.

2.2.4 New Split Process: Ink 19217S

The main disadvantage of the first scale up was the very long grinding times required. Carbon1 was milled for 50 hours in the first step of that process. To lower the grind time, it was realized that the attritor speed needed to be increased. The low viscosity of the mill base in the first scale up trial led to a limit in attritor speed that could be used due to the rise of the liquid level out the top of the grinding flask at higher speeds.

To increase the viscosity of the mill base in this next scale up, the concentration of carbon1 was doubled. A process scheme was developed involving the following steps: 1. Milling carbon1 at double the concentration required in the final ink (other ingredients except water at their normal concentrations); 2. After this initial milling step, rinsing the mill base out of the attritor using the remaining liquid ingredients that would bring the liquid composition up to that of a double batch.; 3. Mixing the output of Step 2 with the other dry carbons needed to bring the composition to exactly that of a double ink batch. Taking half of that double ink batch mixture and grinding for a short period of time. Repeating that step for the other half of the mixture.

In addition to using the higher viscosity mill base described above, the accessory cover for the 750 ml grind flask was also used in these runs. This provided further assurance of avoiding overflow of the mill base out of the top of the grinding flask. Figure 1 shows the attritor configured in this way. By this method it was possible to run the attritor closer to the maximum speed of 1800 RPM, motor speed, or 1177 feet/minute tip speed. This is three times faster than the maximum speed when using the small attritor flask. The operating condition being used is not one that was recommended by the manufacturer of the attritor but is made feasible with the modification made to the attritor flask.

The first ink formulation for this operating mode was 19217S. Milling of carbon1 was carried out for a period of 23 hours and the other carbons were added at the end of that period and milled for an additional one hour. The ink was removed from the attritor via the bottom drain port of the flask. The ink was very fluid at this stage and flowed very easily out of the flask into a one-gallon bottle. The ink was processed through the additional dispersion step and filtered through a 5 μ cartridge filter. Some properties of this batch at various stages of the process is given in Table 5. The ink was print tested and found to be equivalent to the previous Type 6 inks made by different processes. In the end, this process yielded about 6 kilograms or about 5 liters of ink.

Table 5: Properties for Ink 19217S

Mix/Ink	Particle Size Distribution (nm)				R _s	Sample Description
Attritor #/Ink	SSA (m ² /g)	D10	D50	D90	Ω/\square	Details
19217S	12.4	0.172	1.314	11.22		1 hr milling
19217S	38.2	0.069	0.214	3.066	94.5	19 hr milling
19217S	55.5	0.053	0.138	1.053	81	24 hr milling
19217S	46.8	0.058	0.172	3.217	152	Cosolvents added to dilute
19217S	56.6	0.052	0.132	1.222	233	Batch A 1.5 hr milling (carbons added)
19217S	57.2	0.052	0.128	1.345	199	Batch A 2.5 hr milling
19217S	49.0	0.056	0.165	2.469		Batch B 1.2 hr milling (carbons added)
19217S	50.5	0.054	0.180	2.643	190	Batch B 2 hr milling
19217S	58.9	0.051	0.122	0.916		Batch A + B
19217S-D	61.5	0.052	0.108	0.715	234	Dispersion Step
19217S-D5F	59.4	0.051	0.123	0.933	208	5 micron filtration/5070g (81.9% yield)

2.2.5 Scale Up to Produce 6 Gallons of Type 6 Ink

With this new, split process, qualified by the successful production, characterization, and printing of batch 19217S, work began very quickly to prepare a 5 to 6 gallon quantity of this ink as requested by management. This scale up was planned to consist basically of 4 separate attritor cycles prepared similarly to the split process used with 19217S. After each attrition run was characterized extensively, they would be combined into one large masterbatch that would be taken through the additional dispersion and filtration steps as one large batch.

The attritor milling conditions are shown in Table 6. The attritor is run at the lower speed for an hour and then the speed is increased for the rest of this initial run with the carbon1 pigment. After this material is flushed out of the attritor with the additional ink liquids, the other carbons are added to this output and thoroughly mixed. The entire amount is then split into two, with the two parts designated as Batch #1 and Batch #2. Each of these are attritted for an additional 1-3 hours at the lower RPM setting.

In an ideal production scenario and with the right processing equipment, it is envisioned that the four 19217S-like batches could be completed through the attrition step in a single week. This would require completion of that first of four 19217S-like batches on the second day of the run and starting the second batch before the end of that day. Using this cycle, four runs can be made in a work week if the process is started on Monday morning and the workday is extended by about 2 hours. This would provide nearly 25 kilograms or 6.3 gallons of material for further processing in the additional dispersion step, before processing losses. However, the four runs described in this section were not made in a single week. Rather, each run was made over a separate two-day cycle extending over a three week period.

Table 6: Attritor Milling Schedule

		Attritor Setting	Tip Speed
Process	Hours	RPM	Feet/Min.
carbon 1 milling	1	1400	915
	19	1600	1046
	23-24	1600	1046
Batch #1	1-3	1400	915
Batch #2	1-3	1400	915

The four lots prepared in this large scale up were designated as 19240-S, 19246-S, 19248-S, and 19252-S. Tables 7 through 10 contain property data for each of these batches prior to their being mixed as a masterbatch for the additional dispersion and filtration steps.

Table 7: Properties for 19240-S

Mix/Ink	Particle Size Distribution (nm)				R _s	Sample Description
Attritor #/Ink	SSA (m ² /g)	D10	D50	D90	Ω/□	Details
19240S	11.9	0.178	1.441	12.998	277	1 hr milling (1400 RPM)
19240S	43.4	0.060	0.208	2.655	90	19 hr milling (1600 RPM)
19240S	44.3	0.059	0.210	3.664	86	23 hr milling (1600 RPM)
19240S	48.0	0.056	0.182	3.341	244	Batch 1, 1 hr milling (1400 RPM)
19240S	48.7	0.058	0.188	1.895	185	Batch 2, 1 hr milling (1400 RPM)
19240S	45.3	0.058	0.232	4.382	189	Batch 1 + 2

Table 8: Properties for 19246-S

Mix/Ink	Particle Size Distribution (nm)				R _s	Sample Description
Attritor #/Ink	SSA (m ² /g)	D10	D50	D90	Ω/□	Details
19246S	10.4	0.224	1.449	15.915	272	1 hr milling (1400 RPM)
19246S	15.5	0.135	0.989	11.017	180	3 hr milling (1600 RPM)
19246S	1.4	0.125	0.941	8.812	119	6 hr milling (1600 RPM)
19246S	45.0	0.059	0.206	4.134	73	24 hr milling (1600 RPM)
19246S	50.5	0.055	0.164	3.119	180	Batch 1, 2.5 hr milling (1400 RPM)
19246S	50.4	0.054	0.177	3.088	179	Batch 2, 2.5 hr milling (1400 RPM)

Table 9: Properties for 19248-S

Mix/Ink	Particle Size Distribution (nm)				R _s	Sample Description
Attritor #/Ink	SSA (m ² /g)	D10	D50	D90	Ω/□	Details
19248S	11.5	0.191	1.354	15.518	240	1 hr milling (1400 RPM)
19248S	14.6	0.148	0.973	9.714	167	3 hr milling (1600 RPM)
19248S	17.5	0.118	0.854	8.105	122	6 hr milling (1600 RPM)
19248S	45.7	0.058	0.205	3.884	70	24 hr milling (1600 RPM)
19248S	50.8	0.054	0.164	2.964	206	Batch 1, 2.5 hr milling (1400 RPM)
19248S	47.3	0.056	0.224	3.058	162	Batch 2, 2.5 hr milling (1400 RPM)
19248S	52.7	0.053	0.167	1.519	171	Batch 1 + 2

Table 10: Properties for 19252-S

Mix/Ink	Particle Size Distribution (nm)				R _s	Sample Description
Attritor #/Ink	SSA (m ² /g)	D10	D50	D90	Ω/□	Details
19252S	11.8	0.184	1.387	16.645	237	1 hr milling (1200 RPM)
19252S	14.3	1.023	1.023	10.597	187	3 hr milling (1600 RPM)
19252S	21.0	0.102	0.739	8.883	126	6 hr milling (1600 RPM)
19252S	43.7	0.059	0.244	4.762	74	24 hr milling (1600 RPM)
19252S	49.5	0.055	0.167	4.191	208	Batch 1, 2.5 hr milling (1400 RPM)
19252S	51.6	0.054	0.161	3.362	181	Batch 2, 2.5 hr milling (1400 RPM)
19252S	55.9	0.052	0.137	1.261	179	Batch 1 + 2

The particle size distributions (PSD's) for ink 19248-S for various times of attritor milling are shown in Figure 7. All four ink lots that went into the masterbatch showed nearly identical behavior.

After the other carbons were added, the PSD's were measured again and are shown in Figure 8. The curves labeled B1 and B2 are the first and second lots prepared from the dilution of the milled carbon. The curve labeled B1 + B2 is the mixture of the two lots.

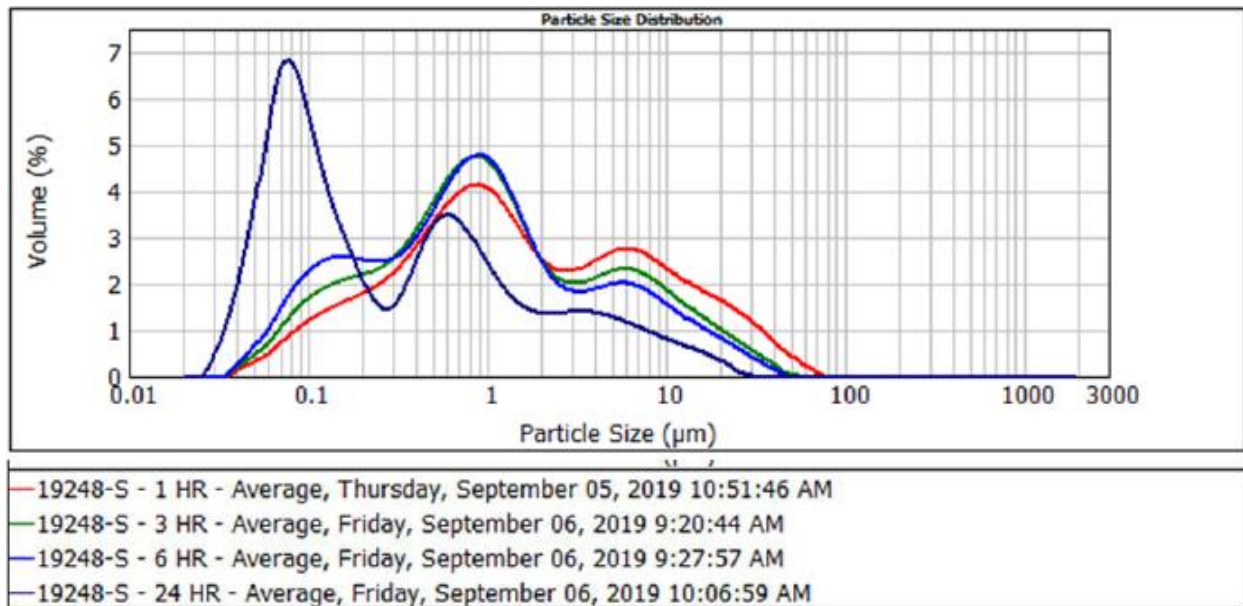


Figure 7: Particle Size vs. Milling Time of 19248S before addition of other carbons

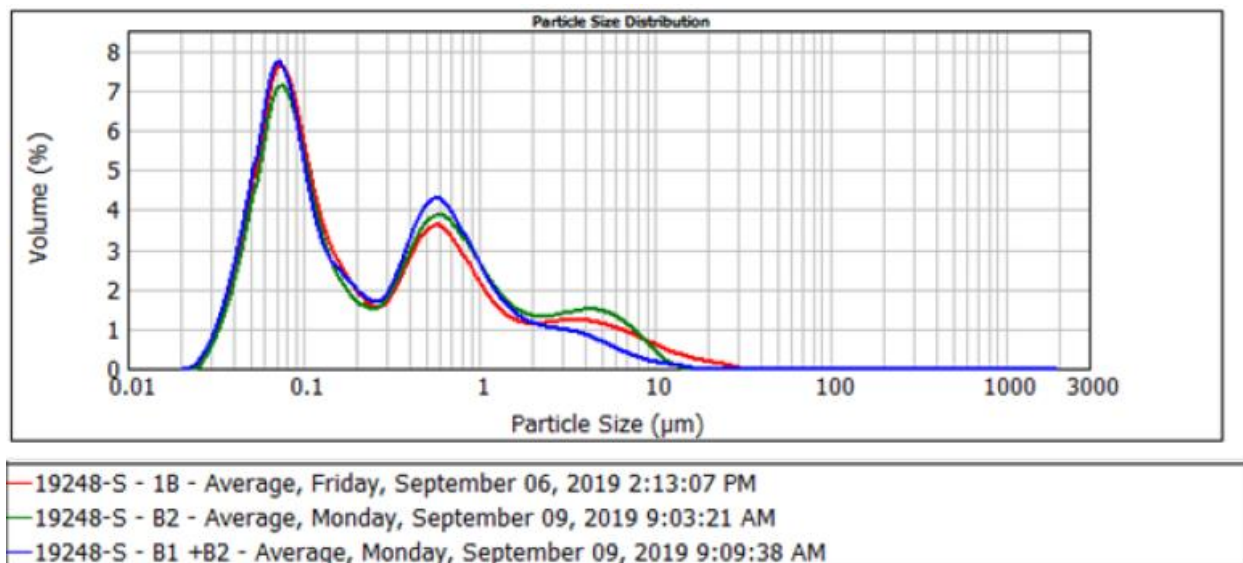


Figure 8: Particle Size of 19248S after other carbon addition and milling

It took approximately one hour to process each gallon of ink through the additional dispersion step. As each gallon was completed, filtration was initiated by pumping through a Meisner 10 μ cartridge filter. Previous batches had been filtered through a 5 μ cartridge filter but that was found to require two filters per gallon. Based on little difference seen in the PSD before and after filtering, it is theorized that the filter media is not fully compatible with the ink and that is causing the filter failure, not particles being filtered out.

After the first gallon of ink was filtered, the PSD was measured and compared to the ink before filtering. The ink was also tested in the experimental lab printer. The results of both tests indicated acceptable ink performance so that all the ink continued to be processed.

After all the completed operations, the ink making process yield was calculated and is shown in Table 11. The starting total of the combined ink lots was 24.771 kilograms and the final recovery was 21.596 kilograms or 87.2% of the starting material. Considering the ink loss from each of the process steps that required ink transfer from one container to another, the yield for this batch was considered acceptable. Some improvement would be expected with minor modifications. Some of the loss can also be attributed to extensive ink sampling for PSD, physical properties, and printing that was not considered in the calculations.

The recovery from the attritor processing is the lowest at 91.1% and is to be expected since the separation of the ink from the milling media is difficult. The combined yield for the additional dispersion step and filtering was 94.7%. Most of this loss is the result of ink transfer to the additional dispersion step and ink lost in the filter cartridge.

The surface resistance of the milled ink was measured from coatings on polyglass made with a #5 Meyer Rod. The measurements of three of the lots are shown in Figure 9. The process is very reproducible and shows the minimum resistance value of 70-86 Ω/\square after 24 hours of milling. The milled lot was then diluted and the additional carbon powders were added to the batch and mixed. This was then split into two separate mixes that were then attrited for another 2.5 hours. The data points shown at 26.5 hours represent those samples. The "ink" at 24 hours is very viscous and not acceptable for jetting. Dilution of the ink after the first step to reduce viscosity will produce a jettable ink, but one that will gel in a few hours. The addition of the other carbons appears to stabilize the viscosity of the ink but with a loss of conductivity as shown in Figure 9.

The PSD of each of the ink lots that made up the masterbatch was monitored by sampling the ink at each point. Data for three of ink lots are plotted in Figures 10 and 11 for D90 and D50 particle size parameters, respectively.

The first and last gallon of the final filtered ink were measured for PSD as shown in Figure 12. The red curve is the PSD for the masterbatch that comprised the four separate ink lots before the additional dispersion step. The green and blue curves represent the measurement of the first and last gallon of ink after the additional dispersion step and filtering through a 10 μ Meisner cartridge filter.

Table 11: Ink Process Yields

Ink Lot #	Net Mass	% Net
19240	5709.0	92.2
19246	5599.8	90.4
19248	5726.9	92.5
19252	5768.0	93.1
Lots Total	22803.7	92.1
T6 -B#1	21596.0	94.7
Total Lot	24771.2	87.2

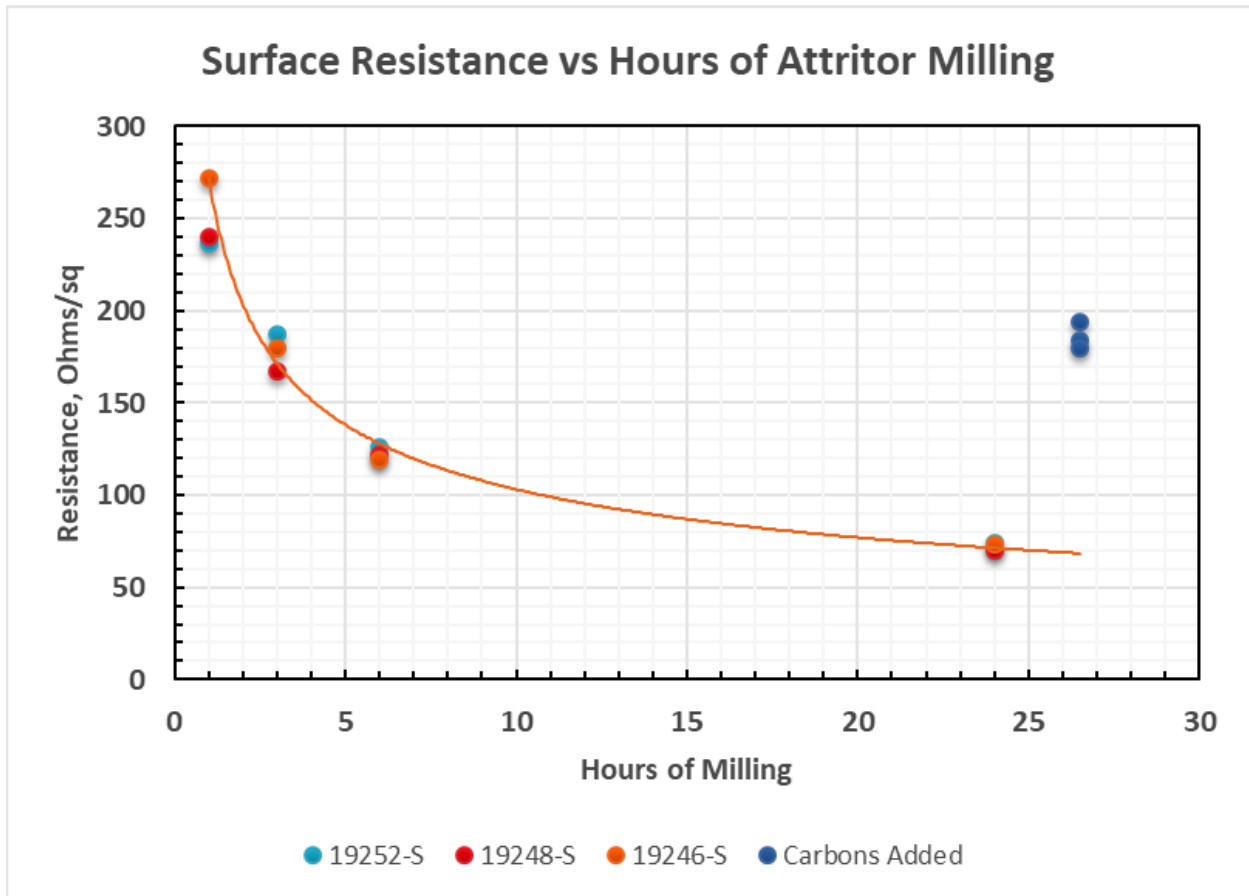


Figure 9: Surface Resistance of Three Ink Lots vs. Hours of Attritor Milling.

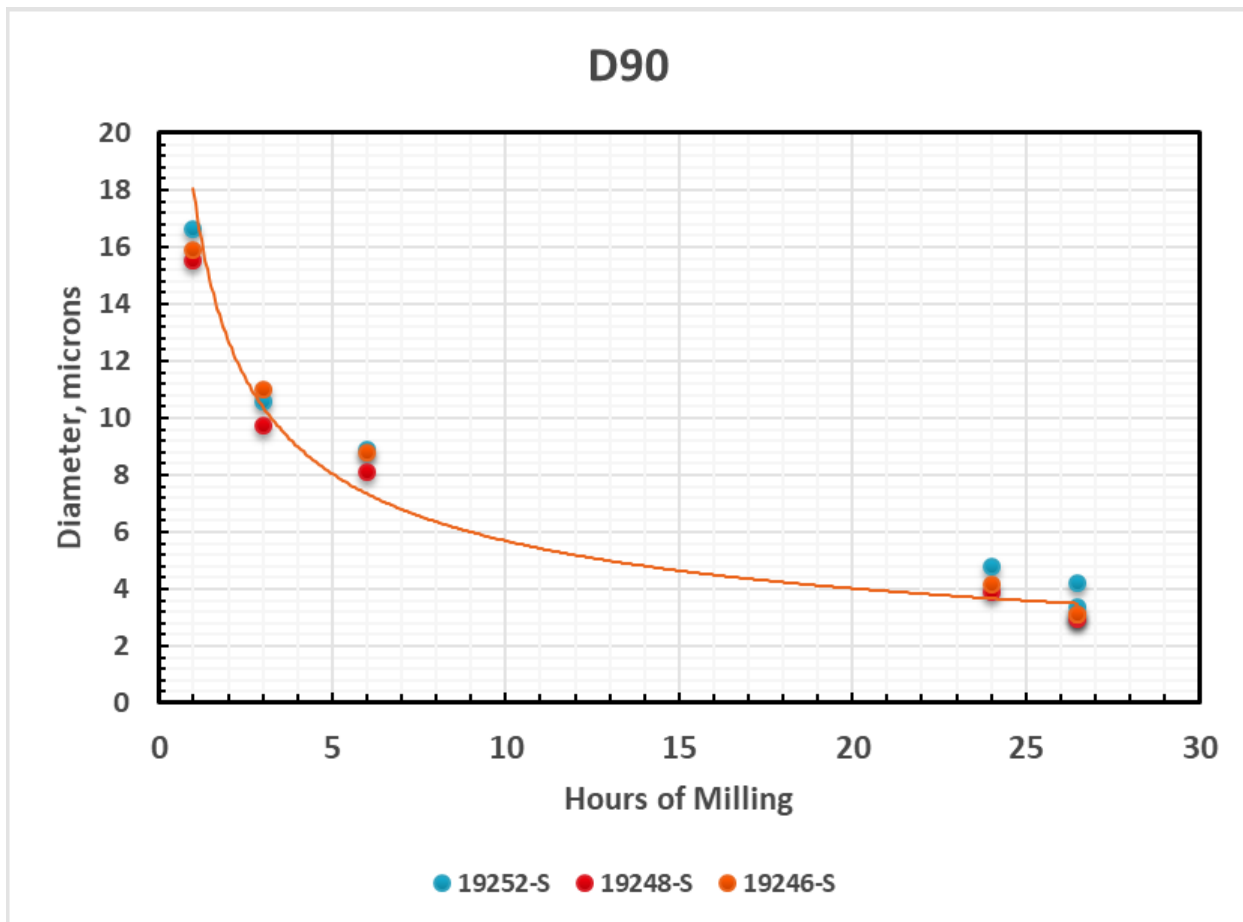


Figure 10: D90 Particle Size of Three Ink Lots vs. Hours of Milling

The physical properties of the final completed ink, designated Type 6, Batch #1, were measured and are shown in Table 13. Properties fall in the range of very functional printing inks in Dimatix heads. This type of ink formulation has been found to age towards higher viscosity at room temperature which can accelerate at temperatures over 35°C. The rate of aging was observed to depend on the specific ink composition and processing conditions. The current scaled up formulation was selected to minimize aging but aging was not studied in detail since a large amount of ink is required to do so. Characterization of this aging must be done for the current formulation and processing in the future. In the meantime, this ink supply is being chilled and properties are being periodically checked. The ink inventory is refrigerated at about 8°C until placed in use.

The printability of the T6 ink was evaluated in the Experimental Print Fixture. Ink was loaded into the printhead and printing was done over a period of several days to look for functional issues. The ink was also used to print several test patterns of interest. All printing was on the substrate supported by a platen heated to 65°C.

D50

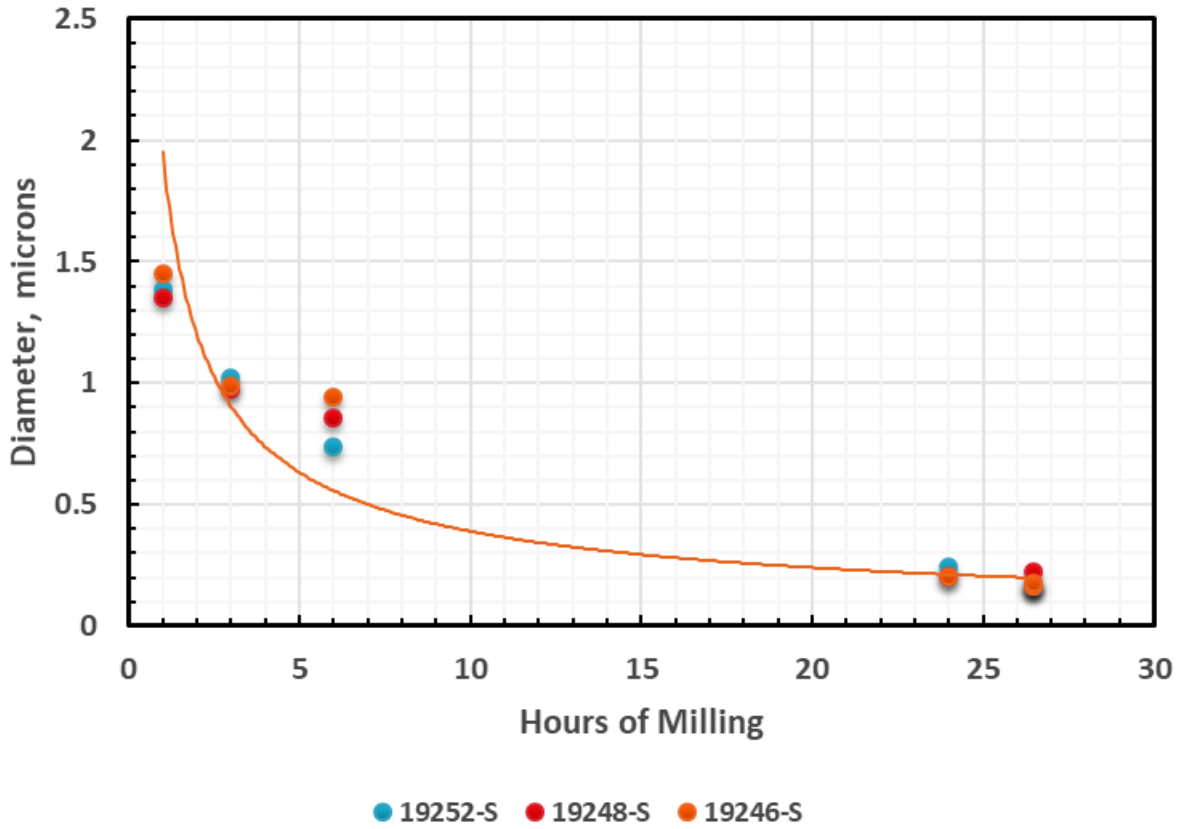


Figure 11: D50 Particle Size of Three Ink Lots vs. Hours of Milling

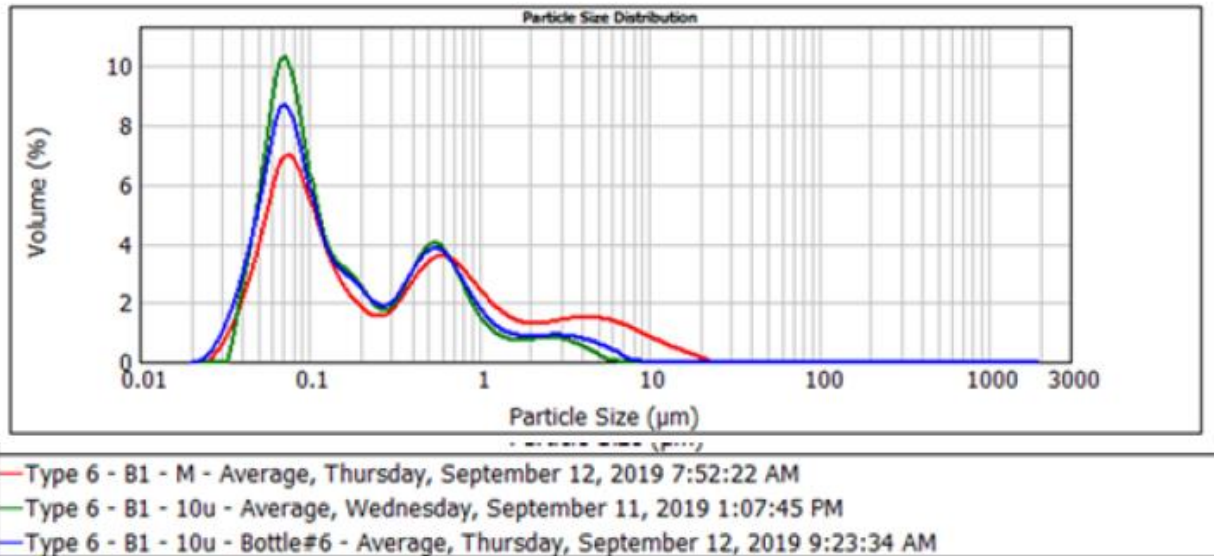


Figure 12: PSD after the dispersion step and final filtration, first and last bottles

Table 14 shows some solid area print data on polyglass substrates. A comparison is made between ink 19217-S, the original scaled-up composition made by split processing, and Type 6, Batch #1. The results are well within measurement variation.

Figure 13 shows the viscosity dependence on temperature for ink 19217-S that had been refrigerated for about two weeks. The ink was allowed to rise in temperature over several hours while undergoing continuous viscosity measurements. The central data points are actual measurements while the 15°C and 25°C points are extrapolations based on the linear best fit line generated from the data. This data was provided to help in understanding the shift in printed resistance on a production printer over a long print run. The ink viscosity drops about 0.5cps for every 1°C increase in temperature.

Table 13: Type 6, Batch #1 Physical Properties

Viscosity	Surface Tension	Solids	PSD		
			SSA	D50	D90
cps @ 25 °C	Dynes/cm	%	m ² /g	D50	D90
13.23	41.1	16.4	57.7	0.128	1.213

Table 14: Printed Surface Resistance Produced on Polyglass (Ohms/Sq.)

Inks	Comments	Solid Area 25% Coverage			Solid Area 50% Coverage		
		1 Pass	2 Passes	3 Passes	1 Pass	2 Passes	3 Passes
19217-S	Initial formulation/Process	1082	275	162	220	85	
T-6 Batch #1	Batch made from 4 combined ink lots	1080	302	157			

The T6 ink being used in a production printer ink tank was sampled and the particle size distribution measured. Figure 14 shows the results that appear similar to the starting ink and 19217-S.

2.2.6 Conclusions and Next Steps for Scale Up of Type 6 Ink

The results presented in this report show that a scaled up process for producing Type 6 ink was successfully demonstrated. The ink can now be made in multiple kilogram or gallon quantities in a timeframe that is consistent for now with production printer demands. The quality and performance of the scaled up ink has been shown to be equivalent to inks made during the initial formulation work and early experiments with smaller scale attritor batches. The performance of this ink has been confirmed to be a significant improvement over previous inks.

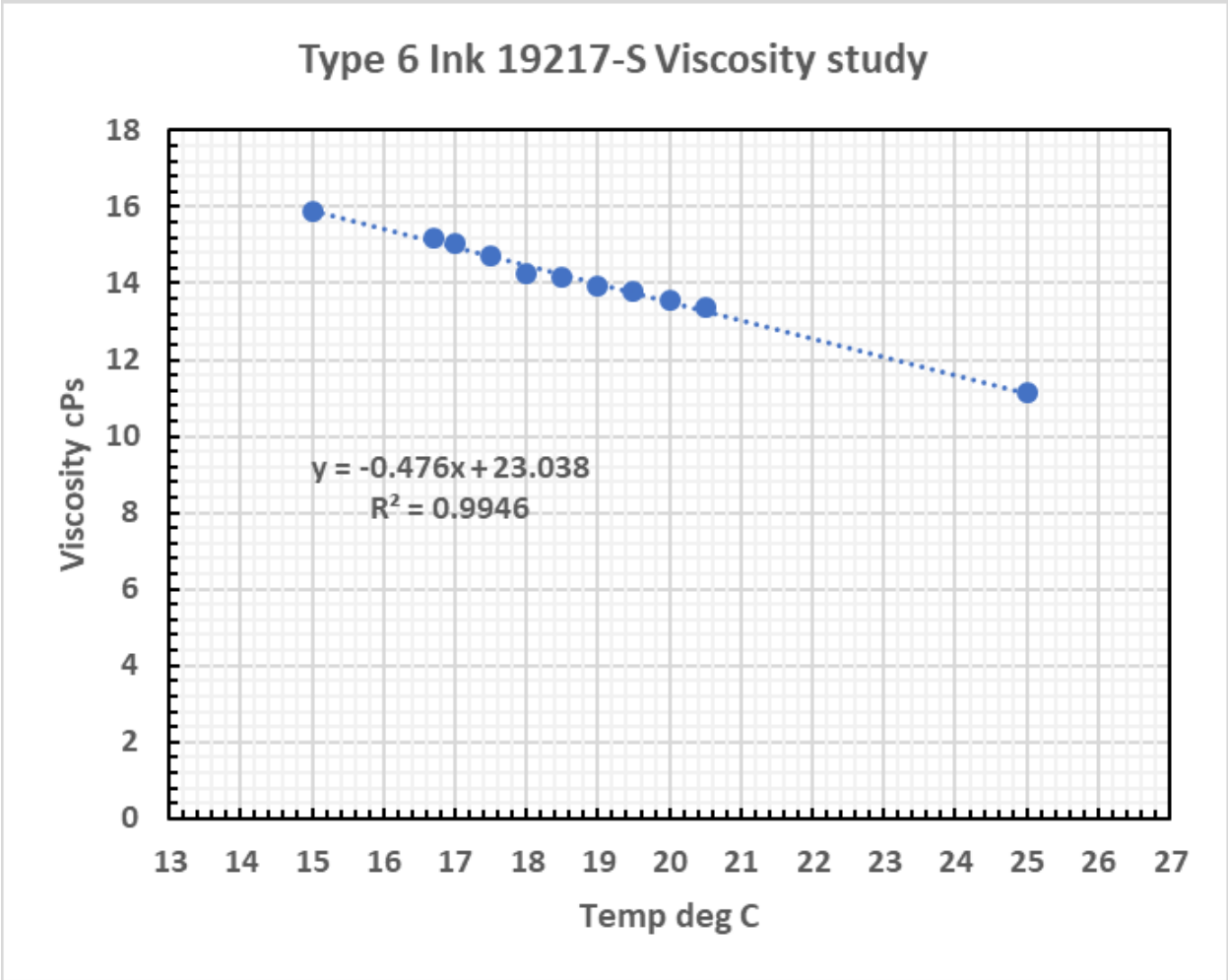


Figure 13: Type 6 Ink 10217-S Viscosity Dependence on Temperature

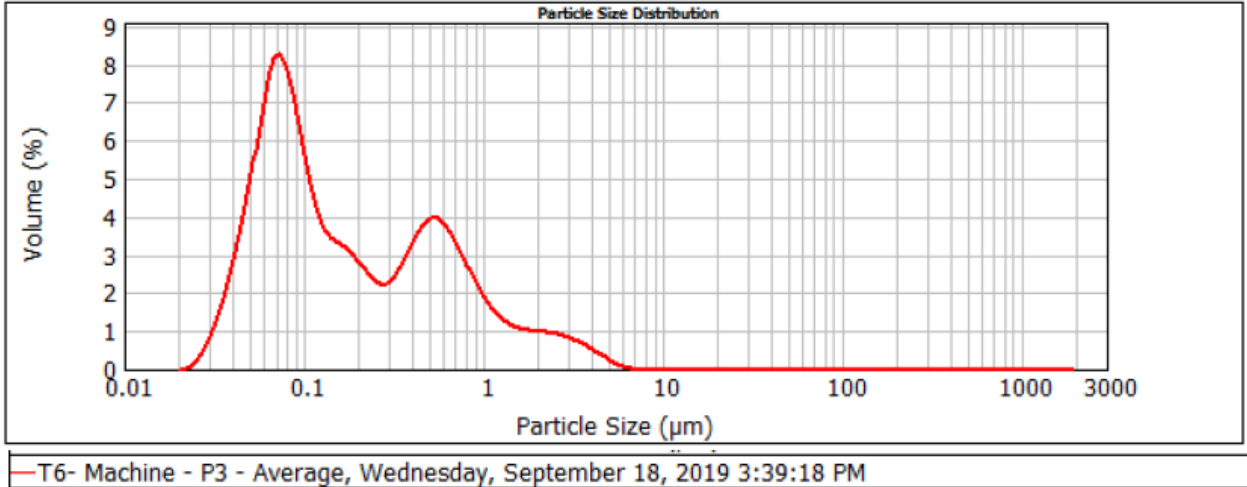


Figure 14: Particle Size of T6 Ink Sample Removed from Production Printer

Areas for further exploration include working toward a better understanding of the aging of this ink formulation and how that is impacted by storage temperature. Although not planned, further study of the rheology of some of the formulations made in the course of this work would be very interesting.

2.3 Objective 2: Next Generation Ink Design

2.3.1 Background

While the refining of the Type 6 process was taking place, work began on the next generation ink design. Over time, forms of carbon that had previously been excluded from consideration due to price and availability now were found to be more readily available at more reasonable prices. Acquisition of samples of one new form of carbon, henceforth called carbon2, began roughly in June and initial formulation work was started in mid-July. Candidate formulations were processed using the 750 ml grinding flask which conserved material while creating 300-400 ml of ink for evaluation. The final formulation has virtually achieved the stated goal of the project which was to hit a sheet resistance of 10 ohm/square with only three passes of printing.

2.3.2 Material Selection

To generate a very conductive carbon layer it is advantageous to use larger carbon particles having fewer particle-particle contacts, especially in the presence of the necessary polymeric binder. There has been a long-term effort to source carbon blacks having a basic particle size in the fractions of a micron rather than in the nanometer range. The issue with that approach is that most carbon blacks are produced for their covering power and dispersibility. The larger carbon blacks tend to be slated for inclusion in rubber compounding for tires and the need for thermal stability. Those carbon blacks tend to be less chemically pure and lower in conductivity. A new form of carbon, carbon1, was found that was first incorporated in the Type 5 ink design and that is larger in particle size than carbon blacks. Type 6 was a further improvement enabled by the milling process developed to achieve better control over the size of carbon1. Both inks require the addition of other carbons to produce highly conductive layers. The other carbons probably fill the voids between the larger particles of carbon1, whether it is milled or not.

Inks in this series were also developed with the goal in mind to scale the formulation up as demonstrated in the previous section with Type 6. This has provided additional constraints on forms of carbon to be considered. The material should be available in kilogram quantities, with consistent properties, and at reasonable prices. While there are many exotic forms of carbon with high conductivity that have become available recently, very few could be considered against these criteria. This work was enabled by newly affordable carbon, henceforth called carbon2, available in large volumes suitable for ink jet ink, allowing for more extensive formulation work.

Throughout this work samples of carbon from many suppliers were evaluated. One product from a specific supplier was chosen for work to proceed, even as alternatives

were still being evaluated. Formulation work started in earnest with the acquisition of one kilogram of what will be called carbon2P1 (for carbon2, Product 1) in late September.

2.3.3 First Ink Formulations

The first formulation was prepared at 12% total carbon with a 2:1 ratio of carbon2P1 to carbon1. The ink was very conductive and the PSD appeared to be in an acceptable range but it was unlike any of the previous ink formulations. The curve was bimodal with one of the peaks at about 1-2 μ . Unfortunately, the ink was found to be unprintable on the printing fixture as ink did not flow through the printhead. A second attempt at 10% total carbon was very successful. It was later determined that the printing issues with the first ink, 19274-G were the result of two issues. The D90 of the final filtered ink was 8.098 μ , much greater than previously tried in the test printhead, and the viscosity was high at 17.3 centipoise. The D90 is believed to have caused clogging of the rock filter in the printhead.

Processing of the sample was initiated by adding carbon2P1 to a beaker, adding the liquid components to the powder, and then mixing with a high speed mixer. The very thick mud-like mix was added to the attritor flask and the attritor started. Milling was continued for 28 hours, at which point carbon1 was added and milling continued for another 3 days. The sample was extracted from the milling media and processed through the additional dispersion step. Ink PSD and surface resistance was monitored at various stages in the process and the results can be seen in Table 15.

The initial step in the ink making process consisted of milling the formulation with only carbon2P1 as the pigment. This composition was designated 19275-G. After carbon1 was added, the material was labeled 19277-G. After 28hr of milling, the carbon2P1 material produced a drawdown resistance value of 179 Ω/\square , a very encouraging value, but the D90 of 37 μ was much greater than target. Within a half hour of adding carbon1, the resistivity decreased to 59 Ω/\square . After three days of milling, the D90 dropped to 13.6 μ and the resistance was 86 Ω/\square . After final processing (additional dispersion step and filtration), the ink had a D90 of less than 5 μ and a resistivity of 108 Ω/\square and was considered a great success.

A 125g sample of 19277-G ink (filtered through a 1 μ glass syringe filter) was provided for print testing. The results were very consistent with the values obtained with Meyer rod draw-downs on polyglass. Table 16 shows the surface resistance values for 1, 2 and 3 pass over printing of a 'solid' image. The values in black text were printed at 25% area coverage and the values in blue at 50% area coverage. Ink spreading at the 25% setting resulted in fairly uniform ink area coverage. In this case, the 25% three coat printing gave the same resistance value as the #5 Meyer rod. It should be noted that there is no image curing between over prints but the substrate is on a platen heated to 65°C.

Table 15: Properties of Inks 19275-G/19277-G

Mix/Ink	Particle Size Distribution (nm)				$R_s, \Omega/\square$			Sample Description
Attritor #/Ink	SSA (m ² /g)	D10	D50	D90	1C	2C	3C	Details
19275-G	0.149	19.829	103.865	235.346	NM			Homogenized
	0.174	17.473	74.027	170.362	NM			1 hr milling
	0.6	5.07	16.129	37.087	179	46		28 hr milling
19277-G	0.1	0.823	15.548	41.053	59			0.5 hr milling
	13.3	0.114	3.736	13.613	86	30	18	3 days milling
	27.9	0.084	1.216	3.087	102/93	38/35	23	Dispersion Step
	27.9	0.085	1.223	3.087	108			Filtered

Table 16: Sheet Resistance of Printed Solid Areas of Ink 19277-G

$R_s, \Omega/\square$		
1 C	2C	3C
728/203	195/68	105/39

2.3.4 “Final” Formulation(s)

After the initial success with the first sample of carbon2P1, a second sample, designated carbon2P2 from the same source was acquired. The supplier claims carbon2P2 is smaller in particle size than carbon2P1 by about a factor of two, which should be an advantage resulting in reduced milling time. The new sample is 15-20 times smaller in particle size depending on whether one is comparing D50 or D90. Further ink work was carried out using this smaller sized material, resulting in further reduction of resistance values. It is not clear whether the improvement is the result of the reduced carbon2 size, a different morphology of the material, or ink processing.

Table 17 lists a series of inks made with carbon2P1, carbon2P2, and carbon2P3. Carbon2P3 is a sample of a carbon2 product from a different supplier than that of the previous two carbon2 samples. These inks were made with similar formulations and with a process similar to that described previously for ink 19277-G.

Figure 15 has sheet resistance measurements for #5 bar draw down samples of several inks from Table 17. The samples were cured after the multiple drawdowns were completed. For reference, results for Type 6 ink are shown in the blue curve at the top. The next curve down in red shows the results for the ink made with carbon2P3 from a different supplier. The results are somewhat improved over that of Type 6 but at a much higher cost compared to that of the other inks in the table made with carbon2 from the first supplier. Four additional carbon2 inks formulated with carbon2P1 (19274-G, 19277-G, 19287-G) and Carbon2P2 (19290-G) are shown in the figure to be greatly improved relative to both carbon2P3 (19267-G) and Type 6 ink.

The initial carbon2 formulations were also evaluated for improvement in conductivity relative to the current Type 3, Type 5 and Type 6 inks as shown in Figure 16. The objective was to determine whether this approach would lead to a significant improvement in

conductivity over that of the recently formulated Type 6 inks. Two of the carbon2 inks, one with carbon2P1 (19277-G) and one with carbon2P2 (19305-G) were tested by making coatings of various thicknesses with Meyer rods (#3, #5, #8, #13, #20) on the polyglass substrate. The resulting resistivity data is shown plotted in the left graph in Figure 16. The data was converted to dried ink layer thickness and replotted in the right-side graph. Type 3, Type 5 and two Type 6 inks (Lab and Scaleup) are shown in the figure for reference.

Table 17: Carbon2 Inks and Their Sources of Carbon2

Ink #	Carbon2 Supplier	Carbon2 Product
19267-G	2	P3
19274-G	1	P1
19277-G	1	P1
19287-G	1	P1
19290-G	1	P2
19305-G	1	P2
19309-G	1	P2

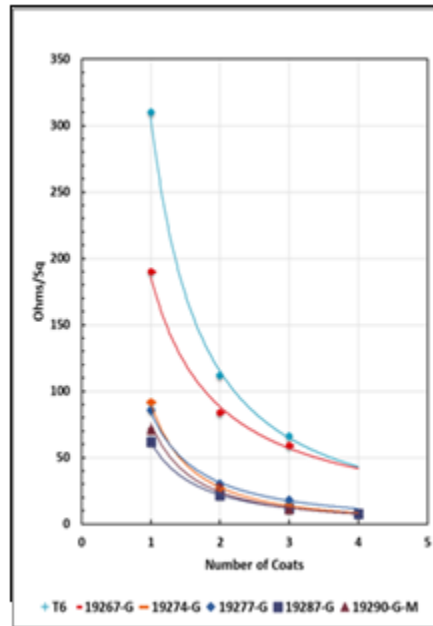


Figure 15: Sheet Resistance vs. # of Coats for Various Carbon2 Inks

The improvement in conductivity of the carbon2 based inks are very dramatic but the results also demonstrate the ink formulated with carbon2P2 shows the most improvement. This performance will have to be maintained to justify the more costly and

processing intensive ink formulation as the ink is being developed further. Experience also predicts some loss in conductivity performance as the ink is scaled up.

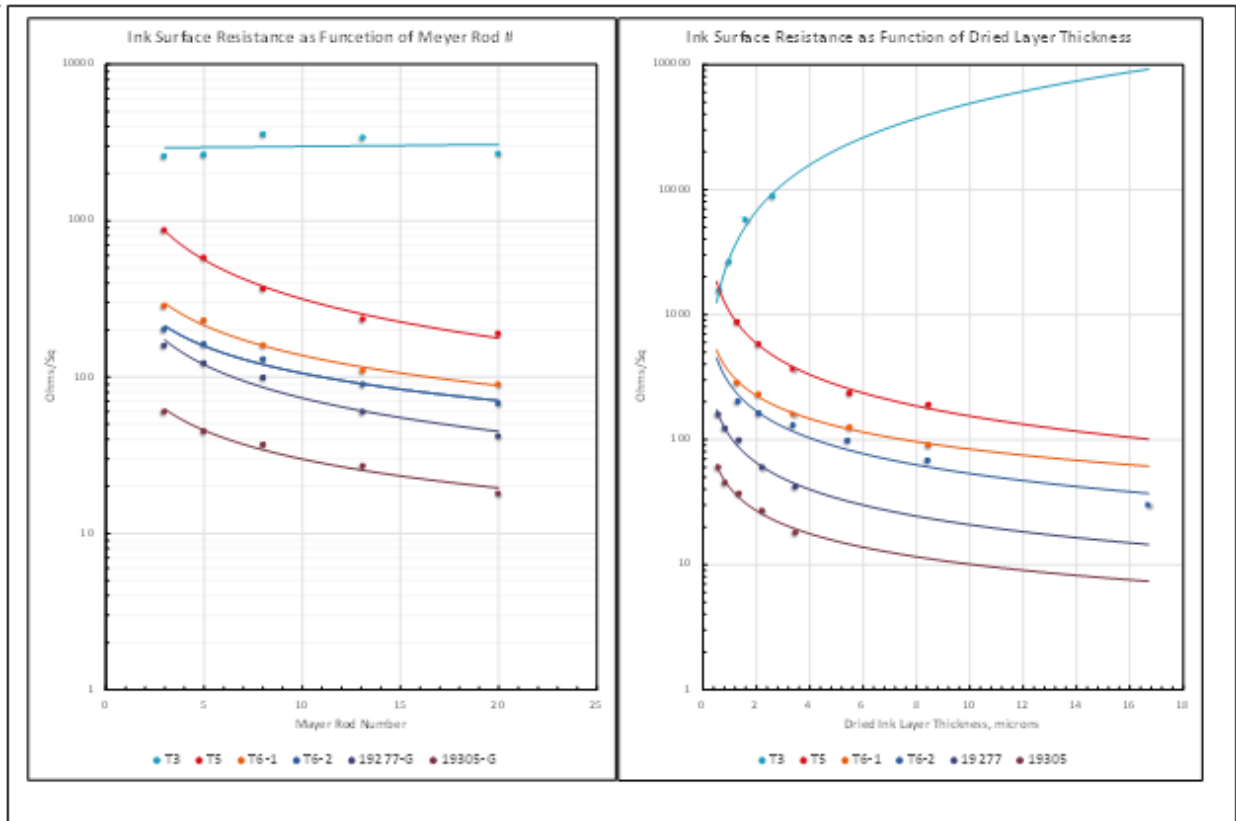


Figure 16: Ink Surface Resistance vs. Coating Rod # (Left Graph) and Surface Resistance vs. Dried Ink Layer Thickness (Right Graph)

Further optimization of the formulation has been ongoing with several encouraging results. Resistivity results for ink 19309-G printed on poly-glass are shown in the following Table 18 that can be compared to those of 19277-G shown previously in Table 16. These values are a result of processing the ink composition with a different milling schedule than that of ink 19277-G. This ink was prepared by attrition of carbon2P2 for 24 hours, adding the milled carbon1 to the mix, and milling an additional three days. The performance of the ink increased by a factor of two.

Table 18: Sheet Resistance of Printed Solid Areas of Ink 19309-G

Rs, Ω/\square		
1 C	2C	3C
376/80	100/29	50/18

2.3.5 Conclusions and Next Steps for Next Generation Ink Design

The results presented in this report also show that a new ink formulation utilizing a new form of carbon has been demonstrated to be a significant improvement over previous carbon ink designs, including Type 6. The performance of this ink is very close to the stated goal of this grant work which was to achieve a sheet resistance of below $10 \Omega/\square$ in three or less passes of printing.

With the carbon2 ink formulation close to being finalized, an attempt was made to place this ink in the context of carbon based inks that have been reported in the literature. Table 19 summarizes in a common format the performance of this latest XACTIV design against seven ink/material systems discussed in a recent journal article by Yu Liao et al.¹

The work in V. Georgakilas et al.^{7,8} (row 6 in Table 19) that used a combination of graphite and chemically modified multiwalled carbon nanotubes showed the highest conductivity among the references cited. The primary referenced paper by Yu Liao et al.¹ claims to have the most conductive materials set. They added carbon black to the graphite, MWCNT-f-OH (dihydroxyphenyl functionalized MWNT) used in V. Georgakilas et al.^{7,8} and waterborne acrylic resins as binders. By extended ink grinding, the graphite in the ink was converted to a few-layer graphene. Their layer thickness was 40μ achieved by screen printing of the ink. They demonstrated that sufficient conductivity to replace silver as the conductive back electrode in an electroluminescent panel was achieved by their formulation. They also claim sufficient conductivity for printed capacitive sensors and flexible wearable electronics.

In Table 19, the results for the XACTIV Carbon2 ink are shown for drawdowns with a #5 Meyer rod, since a theoretical thickness of the dried layer can be computed from the wet layer thickness associated with that bar. It is not as straightforward to get a layer thickness for an inkjet printed image. In Table 20, the results from ink jet printing of that XACTIV ink from Table 19, 20034-GM, are given for one to three passes and for 25 and 50% area coverage. Results are also shown for an even more conductive ink with a higher carbon loading, 19309-GM. Although this ink is still functional, the lower sheet resistance comes at the price of higher viscosity and the requirement for more maintenance of the printhead.

Carbon2 ink 20034-GM, shown in Table 20 demonstrates a level of conductivity equivalent to amorphous carbon or graphite measured perpendicular to the carbon layers. It is more conductive than the screen printing ink described in reference 1.

Supplier1, the source of the carbon2 used in this formulation, claims a conductivity of $8.00E+02$ to $1.10E+03$ S/cm for their material. That is still an order of magnitude better than the current ink but it does not consider the limitations imposed on the fabrication of that material into a jettable ink. To formulate a jettable ink, milling of the carbon2 to reduce particle size, dispersants to stabilize the ink and polymer to fix the image to the substrate, and addition of a surfactant are required.

Table 19: Performance of Carbon2 Ink Against Carbon Inks Cited in Reference 1

Layer Composition	Reference	Ref Date	Thickness, x10-4 cm	ohms/sq	Resistivity		Conductivity	
					micro ohm m	ohm-cm	S/M	S/Cm
Carbon black/Cellulose	2	2017	9.0	250	2.25E+03	2.25E-01	4.44E+02	4.44E+00
Graphite/Carbon Black	3	2017	6.0	38.7	2.32E+02	2.32E-02	4.31E+03	4.31E+01
			9.5	252.2	2.40E+03	2.40E-01	4.17E+02	4.17E+00
Graphitic nanoparticles	4	2017	25.0	220	5.50E+03	5.50E-01	1.82E+02	1.82E+00
MWCNT/Wax	5	2018	90.0	200	1.80E+04	1.80E+00	5.56E+01	5.56E-01
Gr/Polyamic acid	6	2018	15	26	3.90E+02	3.90E-02	2.56E+03	2.56E+01
Gr/MWNT-f-OH	7, 8	2015, 2008	2.86	25	7.15E+01	7.15E-03	1.40E+04	1.39E+02
Carbon black/Graphite/MWNT-f-OH	1	2019	40	29	1.16E+03	1.16E-01	8.62E+02	8.62E+00
Carbon2/Carbon1/polymeric binder	1 Coat		0.91	110	9.57E+01	9.57E-03	1.04E+04	1.04E+02
			3 Coat	2.36	30	7.83E+01	7.83E-03	1.28E+04
Carbon (amorphous)	9	2019			6.50E+01	6.50E-03	1.54E+04	1.54E+02
Carbon (graphite) // to plane	9	2019			3.50E-03	3.50E-05	2.86E+06	2.86E+04
Carbon (graphite) ⊥ to plane					3.50E+00	3.50E-02	2.86E+03	2.86E+01

Table 20: Sheet Resistance of Carbon2 Inks at 10% and 12% Total Carbon

Ink	% Carbon	Rs, Ω/□		
		1P	2P	3P
20034-GM	10	786*/139**	197/48	97/29
19309-GM	12	376/80	100/29	50/18
		* First number at 25% area coverage.		
		**Second number at 50% area coverage		

It can be concluded is that there is not a fundamental reason that further gains cannot be made based on the intrinsic conductivity of various forms of carbon. Nevertheless, as much as a carbon ink can be further improved, it is still two orders of magnitude less conductive than the metals iron through silver, all of which are in the range of 1-7E+5 S/cm.

In summary, the results of this limited survey show that the Carbon2 ink formulation is at least if not more conductive than some of the most conductive carbon inks reported in the literature. The ink is comparable in conductivity to that of amorphous carbon although the last row of Table 19 indicates that much higher conductivities are potentially achievable. In addition, it is usable in ink jet printing with all the benefits in flexibility and speed that provides.

As with Type 6 ink, future work will also focus on assessments of stability of this ink over time and under different storage conditions.

2.3.6 References

1. Liao, Y., Zhang, R., Wang, H., Ye, S., Zhou, Y., Ma, T., Zhu, J., Pfefferle, L., and Qian, J., “Highly conductive carbon-based aqueous inks toward electroluminescent devices, printed capacitive sensors and flexible wearable electronics”, *RSC Advances*, 2019, **9**, 15184-15189.

2. Santhiago, M., Correa, C., Bernardes, J., Pereira, M., Oliveira, L., Strauss, M., and Bufon, C., "Flexible and Foldable Fully-Printed Carbon Black Conductive Nanostructures on Paper for High-Performance Electronic, Electrochemical, and Wearable Devices", *ACS Applied Materials and Interfaces*, 2017, **9**, 24365-24372.
3. Phillips, C., Al-Ahmadi, A., Potts, S., Claypole, T., and Deganello, D., "The effect of graphite and carbon black ratios on conductive ink performance", *Journal of Material Science*, 2017, **52**, 9520-9530.
4. Hof, F., Kampioti, K., Huang, K. J., Jallet, C., Derre, A., Poulin, P., Yusof, H., White, T., Koziol, K., Paukner, C., and Penicaud, A., "Conductive inks of graphitic nanoparticles from a sustainable carbon feedstock", *Carbon*, 2017, **111**, 142-149.
5. Chen, T.-H., Yeh, Y.-C., and Liao, Y.-C., "Healable and Foldable Carbon Nanotube/Wax Conductive Composite", *ACS Applied Materials and Interfaces*, 2018, **10**, 24217-24223.
6. Sankar Nemala, S., Kartikay, P., Agrawal, R., Bhargava, P., Mallick, S., and Bohm, S., "Few layers graphene based conductive composite inks for Pt free stainless steel counter electrodes for DSSC", *Solar Energy*, 2018, **169**, 67-74.
7. Georgakilas, V., Demeslis, A., Ntararas, E., Kouloumpis, A., Dimos, K., Gournis, D., Kocman, M., Otyepka, M., and Zboril, R., "Hydrophilic Nanotube Supported Graphene-Water Dispersible Carbon Superstructure with Excellent Conductivity", *Advances in Functional Materials*, 2015, **25**, 1481-1487.
8. Georgakilas, V., Bourlinos, A., Gournis, D., Tsoufis, T., Trapalis, C., Mateo-Alonso, A., and Prato, M., "Multipurpose Organically Modified Carbon Nanotubes: From Functionalization to Nanotube Composites", *Journal of the American Chemical Society*, 2008, **130**, 8733-8740.
9. Helmenstine, A., "Table of Electrical Resistivity and Conductivity", ThoughtCo., URL: <https://www.thoughtco.com/table-of-electrical-resistivity-conductivity-608499>, updated June 27, 2019. Accessed April 25, 2020.

3.0 Project 2: Low temperature curing of conductive carbon inkjet inks

3.1 Introduction

Over the years, XACTIV has developed a series of increasingly more conductive carbon inks. To date, all these inks have included components that require a high temperature (> 150 °C) thermal cycle for maximum conductivity. There are many applications for printing of conductive carbon inks on surfaces, particularly flexible surfaces, that cannot tolerate temperatures this high. A goal was set to design new inks with a reduced thermal

requirement, targeting 150°C or less. This temperature is around the maximum that polyethylene terephthalate (PET) clear plastic sheets can take before they experience significant deformation.

Many polymeric dispersants and traditional small molecule surfactants were screened for their ability to stabilize the various carbon pigments. Depending on the dispersant finally chosen, it was also recognized that work to identify a new polymeric binder appropriate for the lower temperature curing might also be necessary.

An alternative path that came up slightly later was to thermally dry the ink layer at a low temperature and subsequently use a flash lamp system to cure any polymer binder. A Xenon X-1100 High-Intensity Pulsed Light System with an LS-845 Linear Stage Photonic Curing R&D System was eventually ordered for this purpose.

3.2 Alternative dispersant systems

Table 1 below lists the dispersants screened in the course of this work. They were evaluated in the context of XACTIV's two latest ink formulations, Type 5 (T5) and Type 6 (T6). Small amounts of the ink major components were prepared at the appropriate concentrations and the dispersants were all added at the same percentage of active ingredient as the control (which consisted of the dispersant system for the current inks). They were all sonicated for 10 minutes and then observed at various times after this processing: 0, 1, 2, 5, 10, 20, 30, 60 minutes, 2 hours, 3 hours, and finally the next day. While this qualitative evaluation would reveal some large differences, it was difficult to resolve many samples and overall to quantify the results.

The last two columns in table 1 show the % change in obscuration during a particle size measurement of each of these samples. The higher the % change, the more the particles settled during the measurement. This was taken as a relative measure of colloidal stability, with the lowest % changes being the most stable dispersions. There are difficulties with this evaluation, not the least of which is that the samples are diluted greatly in preparation for the particle size measurement and this dilution is done only semi-quantitatively. Still, the results correlated with the visual observations of settling in the samples and confirmed that only one or two candidates really were close to the control, these being the polyvinylpyrrolidone (PVP) and the sodium salt of lignosulfonic acid.

An attempt was made to produce a Type 5 ink using the PVP but was unsuccessful. In the Type 6 system attempts were also made to use PVP alone and in combination with other dispersants but these efforts were also not successful in producing an ink as stable as the current formulation and not stable enough for a functional ink. It was around this time that the effort to find a new dispersant system was stopped considering the success that had been achieved by this time in drying and curing the current inks with the new Xenon lamp system.

Table 1: Dispersant candidates and a measure of settling in two ink systems.

Chemical Name	Commercial Name	Supplier/Mfg.	T5	T6
sodium alginate		Sigma-Aldrich	11.7	9.5
sodium dodecylbenzene sulfonate (branched)	Rhodacal DS-10	Solvay	7.9	33.3
sodium dodecylbenzene sulfonate (linear)		Sigma-Aldrich	4.0	20.5
sodium dodecyl sulfate		Sigma-Aldrich	29.2	12.8
cetyl trimethyl ammonium bromide		Sigma-Aldrich	13.7	14.1
lignosulfonic acid, sodium salt (MW 8000)		Sigma-Aldrich	2.7	3.4
Poly-(acrylic acid sodium salt) 45% in H ₂ O		Sigma-Aldrich	23.1	28.9
Poly(sodium-4-styrenesulfonate) (MW 70,000)		Sigma-Aldrich	21.3	20.5
Polyvinylpyrrolidone, K-30		Spectrum		
Polyvinylpyrrolidone, MW 55,000		Sigma-Aldrich	-1.4	-0.8
Control			1.4	1.5

3.3 Drying and curing inks with the Xenon lamp system

After the Xenon lamp system was delivered and set up, there was a several week period in which work focused on finding the optimum running conditions for the system and resolving several problems that came up. Samples were subjected to different intensities of UV light after which they were measured to determine the change in surface resistance relative to the platen dried sample (fixture printing is done on a platen heated to 65 °C). The first part of this study was to determine an intensity of light that gave similar results as standard oven curing (> 150 °C). The initial work was done on Hexcel HexWeb HRH-327. This is a woven glass fiber fabric impregnated with an uncured polyimide resin, henceforth referred to as polyglass. After the appropriate intensity was determined on polyglass, other substrates (Kevlar, PET) were tested with the same process to verify the complete curing.

Drawdowns were made on polyglass using Type 6 ink (19140) and a #5 drawdown bar. They were then dried for a few minutes on hot plate at 65 °C. Surface resistance was measured before and after UV light treatment. After this, the samples were also subjected to the standard oven cure to determine if the surface resistance changed. Since this was the first attempt at using the system, the first objective was to determine level of light needed and to work out other problems that were encountered with handling samples.

The first problem encountered was holding the sample in place. Because of the large amount of air that was being drawn through the system, the sample would blow off the table. This was corrected by placing metal strips along each side of the sample. The second problem was the polyglass would leave a stain on the platen after being hit with light. This was corrected by placing reflective white paper underneath the sample. Later it was determined it was best to pretreat the polyglass at high temperature before doing the draw downs and curing the sample with UV light. This prevented the staining and gave better results. The third problem was that the polyglass had a mottle pattern after UV light curing. This was determined to be because of heat sinking of the sample with the metal platen. This was also corrected by placing the paper underneath the polyglass.

Once these things were corrected, the next step was to determine the correct level of UV light to cure the sample.

There are many parameters to set that impact the level of UV light hitting the sample. After reviewing the system manuals, it was decided to increase the distance of the lamp housing window by placing 25.4 mm blocks under each end of the lamp housing. This changes the focus of the light at the sample. Another change was to set the physical aperture width to 80 mm. This is the maximum opening that can be set. Based on the above numbers, and using 4 pulses, the step size was set to a value that gave an appropriate level of overlap of the light on the sample. The last parameter that needed to be set was the maximum carriage speed. This number comes from a table in the linear stage manual and is determined by the aperture opening and the selected lamp voltage.

The next step was to select the values for the 4 pulses. The intensity of the pulse can be set (in Joules) along with the time delay (in microseconds) before the next pulse. It was believed best to increase the power of each pulse and to increase the time delay between pulses. After some experimenting, the best values for the power and time delay were set by recognizing when the curing of the polyglass sample resulted in surface resistance values very close to those seen with standard oven curing of the sample. The next step was to run some samples to confirm the results.

For polyglass as the substrate, some testing was done with samples pretreated to 500 °F as well as virgin samples. The pretreated samples were less conductive after platen drying than the virgin samples but were more conductive after standard oven curing. Because the virgin samples were leaving stains on the platen, it was eventually decided to work with pretreated polyglass samples only. The optimum pretreated sample had a platen dried surface resistance of around 330 ohms and a cured value of 183 ohms, using the bar meter. These values were used to determine if the irradiated samples were close to being cured.

Surface resistance was measured in two ways. One way was with an Extech Model 205 multimeter to which was affixed a plate that held two copper bars, each about 2.5" long and with a 1/4"x1/4" cross sectional area. The bars were parallel and held 2.5" apart. Each was hard wired to connect to one of the inputs to the meter which was operated to read in ohms. In the tables of data to follow, this method of measurement is referred to as the bar meter (BM). The sheet resistance was also measured with an "R-Chek" four point sheet resistance meter, model RC 2175 from EDTM. This method of measurement was referred to as the 4-point probe (4P).

The data in Tables 1 through 8 were taken on samples made by doing a drawdown of T6 ink 19140 on the various substrates using a #5 bar. The initial measurement is after a few minutes drying on the heated platen. Columns labeled "Xenon" mean the data is for samples dried with the Xenon lamp. Columns labeled "2 Xenon" indicate data is for samples sent twice through the Xenon lamp system. Columns labeled "Oven" indicate data is for samples sent through the Xenon lamp and then into the oven for the standard oven treatment. The "shift" is the % difference between the platen dried samples and

whatever other treatment is referenced, for instance, after 1 pass through the Xenon system.

Table 1: T6 ink drawdown on polyglass

Ink#19140 T-6 ink Polyglass							After Xenon		After Xenon and oven	
Sample #20	Initial BM	Initial 4P	Xenon BM	Xenon 4P	Oven BM	Oven 4P	% shift BM	%shift 4P		
1	420	340	238	155	228	143	43.3%	54.4%	45.7%	57.9%
2	368	345	193	150	195	138	47.6%	56.5%	47.0%	60.0%
3	340	339	220	144	192	135	35.3%	57.5%	43.5%	60.2%
4	338	317	168	143	170	135	50.3%	54.9%	49.7%	57.4%
5	325	302	175	132	175	125	46.2%	56.3%	46.2%	58.6%
Average	358.2	328.6	198.8	144.8	192	135.2	44.5%	55.9%	46.4%	58.9%

The results in Table 1 indicate that one pass through the Xenon system seems to be enough. Subsequent standard oven treatment does not reduce the surface resistance very much. For reference, initial work done before this data was taken showed that, using the bar meter, the initial or platen dried sample gave 330 Ω/\square and then 183 Ω/\square after standard oven curing.

Table 2: Repeat of T6 ink drawdown on polyglass by another operator

Ink#19140 T-6 ink Polyglass							After Xenon		After Xenon and oven	
Sample #21	Initial BM	Initial 4P	Xenon BM	Xenon 4P	Oven BM	Oven 4P	% shift BM	%shift 4P		
1	285	307	200	179	196	166	29.8%	41.7%	31.2%	45.9%
2	286	288	166	166	167	158	42.0%	42.4%	41.6%	45.1%
3	270	279	159	148	172	136	41.1%	47.0%	36.3%	51.3%
4	267	301	148	172	150	152	44.6%	42.9%	43.8%	49.5%
5	283	294	170	165	170	158	39.9%	43.9%	39.9%	46.3%
Average	278.2	293.8	168.6	166	171	154	39.4%	43.5%	38.5%	47.6%

These results indicate that, while this drawdown seems have lower sheet resistance than that measured in Table 1, the trends are the same and indicate that one pass through the Xenon system seems to be enough to dry and cure the sample similar to standard oven treatment alone.

Table 3: T6 ink drawdown on pretreated polyglass

Ink#19140 T-6 ink Polyglass							After Xenon		After Xenon and oven	
Sample #22	Initial BM	Initial 4P	Xenon BM	Xenon 4P	Oven BM	Oven 4P	% shift BM	%shift 4P		
1	310	257	216	153	200	137	30.3%	40.5%	35.5%	46.7%
2	295	275	200	150	158	137	32.2%	45.5%	46.4%	50.2%
3	322	256	182	138	167	137	43.5%	46.1%	48.1%	46.5%
4	334	261	165	149	207	136	50.6%	42.9%	38.0%	47.9%
5	289	241	182	131	208	125	37.0%	45.6%	28.0%	48.1%
Average	310	258	189	144.2	188	134.4	39.0%	44.1%	39.4%	47.9%

In this case, pretreating the polyglass seems to have lowered the sheet resistance on both the initial and one pass samples. Only a small change is seen after oven drying the one pass samples.

Table 4: T6 ink drawdown on clear PET film

Ink#19140 T-6 ink Clear plastic							After Xenon		After 2 Xenon	
Sample #23	Initial BM	Initial 4P	Xenon BM	Xenon 4P	2 Xenon BM	2 Xenon 4P	% shift BM	%shift 4P	% shift BM	%shift 4P
1	368	446	200	245	182	240	45.7%	45.1%	50.5%	46.2%
2	363	476	198	255	201	253	45.5%	46.4%	44.6%	46.8%
Average	365.5	461	199	250	191.5	246.5	45.6%	45.8%	47.6%	46.5%

This table has data for the plastic film that cannot take the high temperature oven treatment. The data seems to show that an additional pass through the Xenon system does not lower the sheet resistance significantly, indicating one pass is sufficient.

Table 5: T6 ink drawdown on Kevlar coated with an ink receptive coating

Ink#19140 T-6 ink Powder coat Kevlar							After Xenon		After 2 Xenon	
Sample #25	Initial BM	Initial 4P	Xenon BM	Xenon 4P	2 Xenon BM	2 Xenon 4P	% shift BM	%shift 4P	% shift BM	%shift 4P
1	411	550	220	258	206	242	46.5%	53.1%	49.9%	56.0%
2	422	650	216	304	206	284	48.8%	53.2%	51.2%	56.3%
3	430	703	220	363	210	338	48.8%	48.4%	51.2%	51.9%
Average	421	634	219	308	206	263	48.1%	51.4%	51.1%	58.5%

As seen in the previous table, the data seems to show that an additional pass through the Xenon system does not lower the sheet resistance significantly, although the change in this case is a few percent higher than with the clear plastic film.

Table 6: T6 ink drawdown on virgin Kevlar

Ink#19140 T-6 ink Virgin Kevlar							After Xenon		After 2 Xenon	
Sample #26	Initial BM	Initial 4P	Xenon BM	Xenon 4P	2 Xenon BM	2 Xenon 4P	% shift BM	%shift 4P	% shift BM	%shift 4P
1	448	690	232	365	245	369	48.2%	47.1%	45.3%	46.5%
2	451	673	230	427	237	409	49.0%	36.6%	47.5%	39.2%
3	478	712	253	375	263	372	47.1%	47.3%	45.0%	47.8%
Average	459	692	238	389	248	383	48.1%	43.8%	45.9%	44.6%

The results for virgin Kevlar seem similar to the coated Kevlar. The sheet resistances are higher across the board and the shifts are lower.

Table 7: T6 ink drawdown on Kapton coated with an ink receptive coating

Ink#19140 T-6 ink Coated Kapton, Cured in oven at 500F							After Xenon		After 2 Xenon	
Sample #27	Initial BM	Initial 4P	Xenon BM	Xenon 4P	2 Xenon BM	2 Xenon 4P	% shift BM	%shift 4P	% shift BM	%shift 4P
1	474	538	232	260	220	252	51.1%	51.7%	53.6%	53.2%
2	500	520	204	254	203	252	59.2%	51.2%	59.4%	51.5%
3	468	575	227	290	229	289	51.5%	49.6%	51.1%	49.7%
Average	481	544	221	268	217	264	54.0%	50.8%	54.8%	51.4%

The results for Kapton show an additional pass through the Xenon system gives virtually no change in sheet resistance.

In this case, the results with the bar meter are strange in that the sheet resistance went up with only one pass through the Xenon system. A second pass brings it down slightly

below the initial value. For the 4 point probe, the results are more usual with the sheet resistance dropping after one pass and a second pass does not decrease it any lower. Overall, with this cloth sample, the sheet resistance of the dried and cured samples is not that different from the initial measurement.

Table 8: T6 ink drawdown on cloth material

Ink#19140 T-6 ink Cloth material 12x12 inch material. Take 9 readings for each condition.												
Sample #24	Initial BM			1 pulse Xenon BM			2 pulse Xenon BM					
1	298	202	225	267	252	316	220	187	214			
2	200	232	205	248	240	294	215	196	214			
3	213	210	213	263	317	324	216	216	218			
Average	237	215	214	259	270	311	217	200	215	Shift 1 pulse	Shift 2 pulse	
Grand Average		222			280			211		-26.2%	5.1%	
Sample #24	Initial 4P			1 pulse Xenon 4P			2 pulse Xenon 4P					
1	160	159	170	154	144	164	135	155	171			
2	132	153	158	124	146	146	134	141	144			
3	156	158	189	146	144	162	144	149	164			
Average	149	157	172	141	145	157	138	148	160	Shift 1 pulse	Shift 2 pulse	
Grand Average		159			148			149		7.3%	6.8%	

Samples were then generated in a printer, first with Type 5 ink and then with Type 6. Nine 12”X12” samples were printed of a 100% solid image made with four passes. Table 9 has the initial measurements on these nine samples. Multiple measurements were made around the center of the sample with each meter to gain some statistics. As can be seen in the results, the bar meter gives a lower sheet resistance value but with a higher standard deviation. The 4 prong probe meter has one third the standard deviation of the bar meter on an average that is over 50% higher.

Table 10 shows the results of drying and curing sample #1 using the standard oven treatment. These results are the target values for subsequent samples that will be treated with the Xenon lamp system.

Table 11 has the results for sample #2 which was not air dried before being sent through the Xenon lamp system. The sheet resistances are higher than the control in Table 1. It was noticed that there were many holes in this sample which were the result of the carbon pigment flaking off, apparently due to the loss of solvent which was severe in these samples which were not predried.

Table 12 has the results for sample #3 which was initially treated in a 140 °C (284 °F) oven for 50 minutes. This treatment was seen to evolve a lot of vapor. After this

treatment, the sheet resistance values were close to that of the control. Sending the samples then through the Xenon system gave results very similar to the control.

Table 9: Sheet resistances of printed T5 samples before drying/curing

Bar meter readings BM:									
Sample#	BM1	BM2	BM3	BM4	BM5	BM6		Average	
1	180	227	180	189	171		215	194	
2	173	218	165	210	165		208	190	
3	170	180	180	184	174		190	180	
4	164	190	167	190	156		193	177	
5	156	190	162	195	155		182	173	
6	161	186	156	196	153		179	172	
7	159	192	153	196	153		189	174	
8	162	178	158	174	160		173	168	
9	162	205	161	205	158		204	183	
							Grand average	179	
							Standard Dev	9	
4 Prong Probe readings 4P:									
Sample#	4P1	4P2	4P3	4P4	4P5	4P6		Average	
1	263	285	277	269	283		281	276	
2	261	264	268	266	265		271	266	
3	268	271	274	278	278		284	276	
4	266	266	278	278	278		279	274	
5	275	266	274	276	272		270	272	
6	276	271	285	274	277		283	278	
7	264	278	273	276	271		270	272	
8	281	285	273	266	277		266	275	
9	268	276	279	284	265		275	275	
							Grand average	274	
							Standard Dev	3	

Table 10: Sheet resistances of printed T5 sample with standard oven treatment

Sample #1									
Meter	Reading 1	Reading 2	Reading 3	Reading 4	Reading 5	Reading 6	Average	Initial Values	Target Values
BM	126	125	122	120	122	121	123	194	123
4P	188	193	185	201	191	199	193	276	193
MFB	200	184	182.2	194.5	192	186	190	258	190

Table 11: Printed T5 sample, not dried before one pass through Xenon system

Sample #2									
Meter	Reading 1	Reading 2	Reading 3	Reading 4	Reading 5	Reading 6	Average	Initial Values	Control
BM	153	162	147	153			154	190	123
4P	238	236	254	260			247	266	193
MFB	235.9	248.8	251.9	233			242	258	190

Table 12: Oven dried at 140 °C/50 min. before pass through Xenon system

Sample #3 After oven but before Xenon									
Meter	Reading 1	Reading 2	Reading 3	Reading 4	Reading 5	Reading 6	Average	Initial Values	Control
BM	146	124	139.4	124.5			133	180	123
4P	208	220	208	223			215	276	193
MFB	228	215.9	211.8	230.9			222	255	190
Sample #3 After exposure to Xenon									
Meter	Reading 1	Reading 2	Reading 3	Reading 4	Reading 5	Reading 6	Average	Initial Values	Control
BM	114.9	132	115.4	131			123	180	123
4P	186	191	188	188			188	276	193
MFB	195	186.6	187.6	197			192	255	190

Table 13: Oven dried at 140 °C/25 min. before pass through Xenon system

Sample #4 After oven but before Xenon									
Meter	Reading 1	Reading 2	Reading 3	Reading 4	Reading 5	Reading 6	Average	Initial Values	Control
BM	156	147	150	146			150	177	123
4P	230	233	215	234			228	274	193
MFB	242.7	239.1	229.1	247.3			240	259	190
Sample #4 After exposure to Xenon									
Meter	Reading 1	Reading 2	Reading 3	Reading 4	Reading 5	Reading 6	Average	Initial Values	Control
BM	135.3	128	130.1	118.4			128	177	123
4P	188	193	188	197			192	274	193
MFB	200.1	189.9	196.8	197.5			196	259	190

These results show that 25 minutes of oven heating at 140 °C is still sufficient to enable the Xenon lamp in one pass to dry/cure the sample to a state similar to the high temperature oven control treatment.

Table 14: Oven dried at 140 °C/5 min. before pass through Xenon system

Sample #5 After oven but before Xenon									
Meter	Reading 1	Reading 2	Reading 3	Reading 4	Reading 5	Reading 6	Average	Initial Values	Control
BM	161	156	154	150			155	173	123
4P	266	251	257	255			257	272	193
MFB	258.8	242	253.7	261.3			254	262	190
Sample #5 After exposure to Xenon									
Meter	Reading 1	Reading 2	Reading 3	Reading 4	Reading 5	Reading 6	Average	Initial Values	Control
BM	132	129.6	131.9	128			130	173	123
4P	218	246	247	237			237	272	193
MFB	233.1	211.2	233.2	232.1			227	262	190

These results seem to show that 5 minutes of oven heating at 140 °C may not be sufficient to enable the Xenon lamp in one pass to dry/cure the sample to a state similar to the high temperature oven control treatment. The sheet resistances are close to the control but there were sections of the sample in which the carbon pigment had flaked off.

Sample #6 was left to dry on a 65 °C platen for 25 minutes but there were no changes in the sheet resistance. This sample was then sent through the Xenon system and had a

lot of the carbon pigment flake off. The conclusions drawn were that a 65 °C treatment was not enough to dry the solvents off and, if the solvents are not driven off before being treated with the Xenon lamp, the image will flake off.

Sample #7 was a poor print/bad image and was not used.

Sample # 8 is shown in Table 15 and is a repeat of the control, standard oven treatment. The results were very similar to the control.

Table 15: Repeat of control treatment with Sample #8

Sample #8									
Meter	Reading 1	Reading 2	Reading 3	Reading 4	Reading 5	Reading 6	Average	Initial Values	Control
BM	126.6	125.6	122.8	127.2			126	168	123
4P	186	182	189	188			186	275	193
MFB	187.9	189.3	195	188.4			190	261	190

Table 16: Repeat of 140 °C/25 min. before pass through Xenon system

Sample #9									
Meter	Reading 1	Reading 2	Reading 3	Reading 4	Reading 5	Reading 6	Average	Initial Values	Control
BM	131.9	139.4	134	143.5			137	183	123
4P	191	197	199	203			198	275	193
MFB	204.5	197.9	204	197.6			201	263	190

Sample # 9 is shown in Table 16 and is a repeat of sample #4 and showing similar results.

The overall conclusion was that the ink solvents need to be driven off somehow before passing through the Xenon system or else flaking off of the carbon pigment will result.

Finally, Type 6 ink was used in a printer to print 12”X12” image samples on clear plastic, Kapton coated with an ink receptive layer, and polyglass. This time the image was two passes at 37% solid. Both the polyglass and the Kapton substrates were pretreated in the oven prior to printing.

Table 17 has the results of measurements of the samples after printing and before any drying/curing. The ink did not wet the clear plastic substrate very well. The ink pooled so there are small voids evenly spaced across the sample. Even with the voids, the samples are still conductive although the sheet resistances are the highest and most variable for this substrate.

Table 18 has the results of measurements of one sample of each substrate that we sent for one pass through the Xenon system without any pretreatment in an oven to drive off and ink solvents. No carbon pigment flaked off any of the samples. The clear plastic substrate was slightly distorted due to the heat.

Table 19 shows the results when a coated Kapton and a polyglass sample are subjected to the standard oven treatment. The results show that the sheet resistances are actually

higher than those measured for corresponding samples of the same substrate sent only for one pass through the Xenon system in Table 18.

Table 17: Sheet resistances of printed T6 samples before drying/curing

After printing and before curing:					
Bar meter readings BM:					
Sample#	BM1	BM2	BM3	BM4	Average
Clear plastic #1	336	333	329	334	333
Clear plastic #2	371	416	365	412	391
Clear plastic #3	367	515	386	500	442
Clear plastic #4	450	733	436	672	573
Coated Kapton #5	220	228	243	242	233
Coated Kapton #6	223	220	234	219	224
Poly Glass #7	434	403	400	395	408
Poly Glass #8	410	428	443	458	435
4 Prong Probe readings 4P:					
Sample#	4P1	4P2	4P3	4P4	Average
Clear plastic #1	618	720	632	769	685
Clear plastic #2	664	609	611	639	631
Clear plastic #3	594	1000	779	988	840
Clear plastic #4	855	668	909	815	812
Coated Kapton #5	381	381	380	368	378
Coated Kapton #6	380	381	382	382	381
Poly Glass #7	562	574	565	574	569
Poly Glass #8	581	586	605	575	587

Table 18: One pass through the Xenon system with no pre-drying

Sample #2 Clear Plastic							
Meter	Reading 1	Reading 2	Reading 3	Reading 4	Average	Initial Values	% Change
BM	189	220	179	213	200	391	48.8%
4P	332	405	378	322	359	631	43.1%
Sample #5 Coated Kapton							
Meter	Reading 1	Reading 2	Reading 3	Reading 4	Average	Initial Values	% Change
BM	114.4	111.3	106.2	109.3	110	233	52.7%
4P	169	167	179	175	173	378	54.4%
Sample #7 Poly Glass							
Meter	Reading 1	Reading 2	Reading 3	Reading 4	Average	Initial Values	% Change
BM	250	238	250	206	236	408	42.2%
4P	266	261	288	254	267	569	53.0%

Table 20 shows that the sheet resistance lowers further another approximately 2.5% when the treated Kapton and polyglass samples that were sent through the Xenon system are then subjected to the standard oven treatment.

Table 19: T6 printed samples subjected to standard oven treatment

Sample #6 Coated Kapton							
Meter	Reading 1	Reading 2	Reading 3	Reading 4	Average	Initial Values	% Change
BM	135	148	132.9	145.2	140	233	39.8%
4P	210	213	214	216	213	378	43.6%
Sample #8 Poly Glass							
Meter	Reading 1	Reading 2	Reading 3	Reading 4	Average	Initial Values	% Change
BM	263	273	268	264	267	408	34.6%
4P	325	320	320	319	321	569	43.6%

Table 20: One pass through the Xenon system followed by standard oven

Sample #5 Coated Kapton							
Meter	Reading 1	Reading 2	Reading 3	Reading 4	Average	Initial Values	% Change
BM	99.2	117.6	103.5	102.9	106	233	54.6%
4P	172	171	175	174	173	378	54.2%
Sample #7 Poly Glass							
Meter	Reading 1	Reading 2	Reading 3	Reading 4	Average	Initial Values	% Change
BM	212	263	201	223	225	408	44.9%
4P	262	241	258	260	255	569	55.1%

4.0 Project 3: Transparent, conductive silver inks

4.1 Introduction

At the start of this project, XACTIV had experience formulating several kinds of silver inks. Formulations had been made with nanoparticle inks of various sizes. Work was also done with silver nanowires of varying thickness and length. Finally, there was also experience making silver complex inks. These latter inks consist of silver made into a solution soluble form. When applied to a surface and treated properly, the complexing ligands are lost and the silver is reduced to its elemental form on the surface.

The goals for this project were to obtain a surface resistance of less than $10 \Omega/\square$ and as high a level of transparency as possible, preferably 85% or more. Previous approaches printing narrow grid lines using both nanoparticle and nanofiber inks showed that it was not possible to obtain the required conductivity without broadening the lines to the point where the transparency was very low.

Some success was achieved in previous experiments but they involved creating samples by doing drawdowns on transparencies of inks containing nanofibers that were too long to be jetted. For instance, in one case a surface resistance of $6 \Omega/\square$ was achieved using a #8 bar which also resulted in an average transparency of 88%. With a #5 bar a surface resistance of $\sim 33 \Omega/\square$ was achieved with a transparency of $\sim 92\%$.

Given this history, the work on this project had two main thrusts. One was the synthesis of silver nanowires and their formulation into inks while the other was the formulation of

silver complex inks. A few experiments were also tried using thin drawdowns of a silver nanoparticle ink but were not successful.

4.2 Work on silver nanowires

The goal of this project was to try to synthesize and deposit silver nanowire films with higher conductivity and transparency than currently available commercial silver nanowire products. As noted previously, the target surface resistance was under $10 \Omega/\square$ and transparency higher than 85%. The target substrate was ionic coated polyester (ST505). ST505 has a maximum heating temperature of 150°C before it begins to deform.

Silver nanowires were synthesized using various polyol methods.^{1,2,3} The synthesis of very small (less than $3 \mu\text{m}$ in length) wires with a narrow size distribution was attempted. This was unsuccessful, as all methods produced wires that were longer and had broad size distributions (see SEM image in Figure 1). There are not any large-scale synthesis procedures available that give short wires with tight size ranges. Longer wires were sonicated to break the wires down to the desired size. While the length of the wires decreased with increasing sonication time, they also became agglomerated and entangled in clumps and do not produce conductive or transparent films.

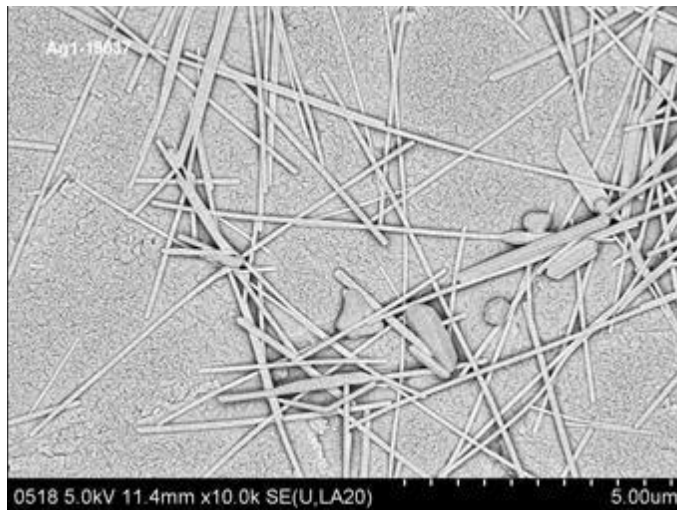


Figure 1: SEM image of synthesized silver nanowires.

Ultra-long silver nanowires ($>100 \mu\text{m}$) were successfully synthesized multiple times (see procedure detailed below). The theory is that longer nanowires require less junctions to create a film (continuous network), resulting in higher transparency and conductivity in the film. These were investigated for drawdown or roll coating, since they are outside the size range of inkjet printing. Using an #20 bar, drawdowns were performed. Even using these materials, it was not possible to achieve less than $10 \Omega/\square$ and over 80% transparency, which is not quite as good as that achieved with commercially available nanowire samples. One reason may be that commercial producers can achieve more pristine wires. Another reason is the ink formulation. The ST505 substrate is very difficult to wet, even with its ionic coating. In addition, the ultra-long nanowires are not easy to

disperse because they are long and heavy. The most efficient additive found to date is a polymer, hydroxypropyl methyl cellulose (2-HPMC), which helps with film-forming. However, this material does not evaporate and is left behind when the ink is dried. Many literature papers can achieve much lower conductivities because they spin coat the wires in ethanol or IPA and therefore no dispersing agents or additives are left behind after curing. Different surfactants, dispersing agents, and additives were sampled from Evonik to improve film properties. None of these were found to improve the film but rather most left the film very resistive, discontinuous, and tacky.

Procedure for Making Ultra-Long Silver Nanowires (ULNW):

Materials:

- PVP (MW: 55,000)
- PVP (MW: 360,000)
- Ethylene glycol, high purity grade
- Silver Nitrate
- NaCl
- FeNO₃·9H₂O
- High temperature range silicon oil
- Circulating Oil bath
- Hot plate
- Oil container
- Calibrated thermometer
- Volumetric pipet
- Stir bar, stir bar remover
- Hot gloves for handling beaker transfers

Perform all reactions in hood, NO₂ gas can result from this reaction and is dangerous

1. Preheat oil baths to 130°C (circulating oil bath system and oil container on hot plate)
2. Add 100mL of ethylene glycol to 250mL beaker with a stir bar.
3. Add 0.32g of PVP (MW:55,000) and 0.32g of PVP (MW:360,000) to beaker and dissolve at room temperature.
4. Add 0.72g of AgNO₃ to solution and dissolve.
5. Separately, create a 30g solution (total weight) with 0.00286g NaCl and 0.0066g FeNO₃·9H₂O in ethylene glycol, dissolve completely.
6. After AgNO₃ has completely dissolved in main solution, add 10mL of FeNO₃/NaCl solution and stir rapidly for 1 minute.
7. Quickly transfer beaker with stir bar to oil bath on hot plate (using steel container to hold oil, see notebook page 2 for setup) and stir vigorously for 10 minutes.
8. After 10 minutes, remove from hot plate oil bath, remove stir bar, and place beaker into circulating oil bath.
9. Carefully cover beaker with watch glass and lay oil bath lid on top (will not fully close but helps keep temperature consistent).
10. Leave for 3.5 hours undisturbed, checking temperature periodically.

11. After 3.5 hours, remove beaker from oil bath and let cool.
12. When cool, add acetone to beaker (to about 250mL line) and let settle. This should crash the wires out to the bottom, since they are coated with PVP that is insoluble in acetone. Collect supernatant and repeat. (Note: if no separation occurs, transfer to larger beaker and use more acetone. Acetone must be in abundance compared to ethylene glycol solution).
13. After wires seem to be clean (two or three acetone rinses), suspend in desired solvent (IPA, water) and collect. (Note: Typically use water, and only added the minimum amount needed to transfer the wires to the scintillation vial. Want to keep as concentrated as possible, it is easy to dilute them later but not to reconcentrate them).

Best Ink Formula for ULNW on ST505 Transparency:

20wt% AgNW concentrate
20wt% HPMC solution (2%wt hydroxypropyl methylcellulose in water)
30wt% water
30wt% IPA

Draw down RDS bar 20, cure for 10 minutes in furnace at 130°C.

Transparency ~80%, conductivity under 10Ω/□

4.3 Work on silver complex inks

An alternative method to obtaining transparent conductive silver films used a silver complex or reactive silver ink method. Several procedures were followed from various patents and papers.^{4,5,6} The primary procedure followed is from a paper by Vaseem et al. detailed below.⁷ Ink was filtered using vacuum filtration. In the paper, the authors state that they were able to store the ink in a refrigerator for up to a month without observing precipitation of solids. However, after following these procedures, precipitation of silver oxide has been observed after leaving the ink sitting overnight and so stability is an issue.

Drawdowns were performed using an # 3 bar on multiple substrates. These included polyglass, coated Kapton, uncoated Kapton, and the transparent ST505 PET (polyethylene terephthalate) film. Films were not conductive on polyglass. Uncoated Kapton and ST505 experienced crawl back (ink not wetting the substrate and pooling together) and did not form continuous films. The coated Kapton produced conductive films with single digit Ω/□ after 3 draw downs.

The ink was printed on ST505 film using an Epson C88+ printer. Thin films were jetted in an attempt to be both conductive and transparent. The ink experienced crawl back and did not produce a continuous film. Therefore, it was not conductive. Future work might involve attempting to source alternative transparencies with more hydrophilic surfaces and/or pretreatment coatings for the transparencies. In addition, surfactants that will improve wettability without hindering conductivity would also be investigated.

Samples of Computer Grafix Clear Transparent Film were evaluated as an alternative substrate. Drawdowns were performed using # 3 bar. After two draw down coatings, the film was conductive but not transparent. The ink was printed on the Epson C88+ printer but did not produce a conductive film with either single or multi-pass prints. It was noted that the coating on the Grafix substrate seemed discontinuous, and when the substrate was wet with water it became tacky. This substrate does not seem suitable for our applications.

Procedure for making reactive Silver ink (MOD ink):

Materials:

- Silver Acetate
- 2M Ethylamine solution in methanol
- Ethanolamine
- Formic acid
- 2-HEC solution (2wt% 2-Hydroxyethyl cellulose [MW: 90,000] solution in 1:1 weight ratio water: methanol solvent, made in advance)
- Water
- Graduated cylinders
- pH meter

Perform all reactions in hood, NH₃ gas and CO gas can result from these reactions

1. Mix 10 mL of ethanolamine and 10 mL of water in a vial.
2. Add formic acid dropwise to the vial until attain a pH of 10.5
3. In another vial, add 1g of silver acetate and 2 mL of ethylamine solution.
4. Shake to wet the silver acetate, sonicate in bath for 2 minutes.
5. Then add 1.5 mL of solution made in steps 1&2 to vial, and 0.5 ml of 2-HEC solution.
6. Swirl, shake and mix until everything is dissolved, may also sonicate in bath for two minutes.
7. Allow to settle overnight, store in dark in fridge (2-8°C).
8. Filter out any particles that form before printing using 0.45µm and 0.22µm filters. (Note: easiest way to do this has been using vacuum filtration).
9. Store ink in fridge when not in use, in dark. Shelf life is limited, particles of silver oxide will form over time.

(Note: Can scale up synthesis, but be aware reaction is exothermic. Mix solutions carefully. The ink has been scaled up to 40 mL successfully).

4.5 References

1. Stewart, I., Kim, M., and Wiley, B., "Effect of Morphology on the Electrical Resistivity of Silver Nanostructure Films", *Applied Materials and Interfaces*, 2017, **9**, 1870.

2. Bergin, S., Chen, Y-H., Rathmell, A., Charbonneau, P., Li, Z-Y., and Wiley, B., "The effect of nanowire length and diameter on the properties of transparent, conducting nanowire films", *Nanoscale*, DOI: 10.1039/c2nr30126a.
3. Prabukumar, C. and Bhat, K., "Purification of Silver Nanowires Synthesised by Polyol Method", *Materials Today: Proceedings*, 2018, **5**, 22487.
4. Kastner, J., Faury, T., Außerhuber, H., Obermüller, T., Leichtfried, H., Haslinger, M. Liftingner, E., Innerlohinger, J., Gnatiuk, I., Holzinger, D., and Lederer, T., "Silver-based reactive inks for inkjet-printing of conductive lines", *Microelectronic Engineering*, 2017, **176**, 84.
5. Mou, Y., Zhang, Y., Cheng, H., Peng, Y., and Chen, M., "Fabrication of highly conductive and flexible printed electronics by low temperature sintering of reactive silver ink", *Applied Surface Science*, 2018, **459**, 249.
6. Mou, Y., Cheng, H., Wang, H., Sun, Q., Liu, J., Peng, Y., and Chen, M., "Facile preparation of stable reactive silver ink for highly conductive and flexible electrodes", *Applied Surface Science*, 2019, **475**, 75.
7. Vaseem, M., McKerricher, G., and Shamim, A., "Robust Design of a Particle-Free Silver-Organo-Complex Ink with High Conductivity and Inkjet Stability for Flexible Electronics", *Applied Material and Interfaces*, 2016, **8**, 177.

5.0 Project 4: Printable semiconductor and electronic devices

5.1 Literature search for material selection

Initially, this project envisioned building P-I-N diodes using a inkjet process. An extensive literature review was undertaken with the goal of identifying materials that might function in such a process. Some of the papers reviewed are listed under the References section at the end of the section for this project. What follows is a summary of the results of that literature review.

P-I-N diodes require three kinds of semiconductor materials: p-type, intrinsic (i-type), and n-type. Usually a device is created by taking an i-type semiconductor like silicon or germanium and doping certain sections to create p-doped and n-doped regions. In terms of printing and solution processing, both silicon and germanium have no record of being solution processed in ambient conditions. Silicon can be acquired from silanes, but that requires all work be done under nitrogen as they are pyrophoric (can spontaneously combust in air). Therefore, other potential routes and materials were sought out as discussed below.

Silicon nanoparticles: Silicon nanoparticles will contain an outer coating of silicon dioxide, unless handled under nitrogen or argon. Thus, even sintering them will be highly unlikely

to result in an amorphous silicon film unless everything is performed in inert conditions and the oxide layer on the particles is etched away before sintering.

Common semiconductor materials: Other common commercial semiconductor materials with comparable performance to silicon semiconductors include cadmium, arsenic, and lead based compounds. They are extremely toxic and undesirable to work with. Attempts to work with any of these compounds would require extensive investments in Personal Protective Equipment (PPE) in addition to special waste disposal arrangements. The toxicity of the compounds makes them unlikely candidates, at least initially.

Metal oxides: A current booming research area is semiconducting metal oxides, such as zinc oxide and nickel oxide. These materials can be solution processed by sol-gel routes and thermal curing. However, the stability of these materials is undesirable. Zinc oxide is light sensitive, and films are brittle. In addition, for p-i-n diodes it is desirable for the i-layer to be the same material as the p- and n- layers, for example, a ZnO i-layer on a p-doped ZnO layer with an n-doped ZnO layer on top. The difference in crystallinity between different oxides (like NiO and ZnO) would make for poor performance. However, there is little literature for any successfully p-doped zinc oxide because it degrades over time after being deposited. No other metal oxides were identified that seem feasible to produce. There seems to be little known about p-type metal oxide semiconductors and those that have been investigated have poor performance or stability. Another issue with semiconductors is that the crystalline or amorphous structure matters. Chemical vapor deposition or a similar process are normally used because of the precision of the structure required. Solution-processed semiconductors do not have that precision, which greatly affects device performance. In addition, any kind of dust or impurity can affect the semiconductor, which is why they are usually fabricated in clean rooms. Attempts to do any kind of metal-oxide research for semiconductors would require extensive investment in outside analytical work. Each sample would need to be sent out for analysis of the crystal structure (X-ray Diffraction, XRD), film formation (Scanning Electron Microscopy, SEM and Energy Dispersive X-ray Spectroscopy, EDS), as well as tested for semiconducting properties (Keithley analyzers). Doping concentrations, film deposition characteristics/parameters, curing temperatures, stability over time after printing, electrical characteristics, and compatibility with other materials to fabricate the device are some of the properties that would each need to be investigated separately and each require a sample be sent out for analysis.

Organics: In general, organic diodes were not investigated because of their lower performance and more fragile stability. However, there appear to be some organic materials that can be used for p-i-n diodes on flexible substrates. This review focused on inorganic semiconducting materials because their expected superiority in performance.

No clear path forward resulted from this literature review. All the systems studied seemed to provide too many challenges. The work did force a closer examination of the problems that would need to be solved to enable fabrication of a device using inkjet printing. Strengths of XACTIV include the ability to reduce materials in particle size and formulate jettable inks with them along with the ability to jet these materials in desired patterns and

layers. However, as noted above, a major issue with semiconductors is that specific crystalline or amorphous structures are required. Just jetting size reduced particles would not result in a usable layer unless they could be sintered or otherwise processed into the desired solid structures.

5.2 Schottky diode using zinc oxide tetrapods

5.2.1 Introduction

After the literature review, a master's thesis by a student in Sweden was brought to the attention of the team.¹ The thesis described the construction of a Schottky diode using screen printing of zinc oxide in the form of commercially available single crystal "tetrapods" (Panasonic PanaTetra). The tetrapods are a form of particulate zinc oxide with four legs extending 10 to 20 microns out from a central core in directions to form a tetrahedral shape.

As explained in the thesis, construction of a Schottky diode with the ZnO tetrapods involves forming contacts with a metal on either side of the semiconductor. A Schottky barrier can be formed when the metal used has a work function higher than the electron affinity of an n-type semiconductor like ZnO. XACTIV has silver inks which are a suitable metal for such a contact as its Fermi level is higher than that of ZnO. Such a contact conducts current in only one direction.

To complete the device, an ohmic contact is made to the other side of the semiconductor using a metal with a work function near or below the electron affinity of the ZnO. XACTIV has carbon inks that have a Fermi level slightly above ZnO. For purposes of demonstrating feasibility of devices, aluminum blocks have also been used to form a temporary contact to the ZnO layer.

5.2.1 Dispersing the tetrapods

Dispersing agents Zetasperse 3800, Tego Disperse 755W, and Tego Disperse 757W from Evonik were tested as waterborne dispersing agents. Four different concentrations (0.5%, 1%, 2.5% and 4%) were tested of each agent with the ZnO tetrapods in water. The Zetasperse 3800 and the Tego Disperse 755W seemed to perform better than the Tego Disperse 757W, but otherwise no detectable difference was observed. The 2.5% and 4% concentrations yielded a less clear supernatant than the lower concentrations for both samples. At the very end of the study, the Zetasperse 3800 appeared to keep the most in suspension.

Sonication tests were also performed. Zinc oxide tetrapods were suspended in water and sonicated for 0.5, 1, 2 and 3 hours. Particle size analysis and microscope imaging were done to observe any size changes. Results showed that the ultrasonic bath was not effective in breaking up the tetrapods. Both imaging with a microscope and particle size analysis did not appear to differ between samples before and after sonication. It was concluded that a higher energy process is needed to break the tetrapods. It is also noted

that the dispersing agent should be minimized so to not affect the semiconducting properties of the ZnO tetrapods and their subsequent films.

5.2.2 Size reduction of the tetrapods

The zinc oxide tetrapods as received have legs of 10 to 20 microns in length extending from a center core. For use in ink jet, these tetrapods need to be reduced in size. Most of the work in this report was done using tetrapods that were milled in a Union Process 01 attritor.² In one run, 19226, the mill base was simply the tetrapods mixed at 25% by weight in isopropanol. Figures 1 and 2 below show the D50 and D90 particle size parameters as a function of time in the attritor as measured on a Malvern Mastersizer 2000. The raw data is given in Table 1.

Table 1: Particle Size of 19226 as a function of attrition time.

(Hours)	D50 (microns)	D90 (microns)	SSA (m2/g)
0	7.606	20.006	1.56
0.083	4.210	11.023	2.36
1	3.925	9.146	2.19
2	3.560	8.504	2.44
4	3.605	8.040	2.33
23	3.100	6.472	2.44
48	2.420	4.604	2.90

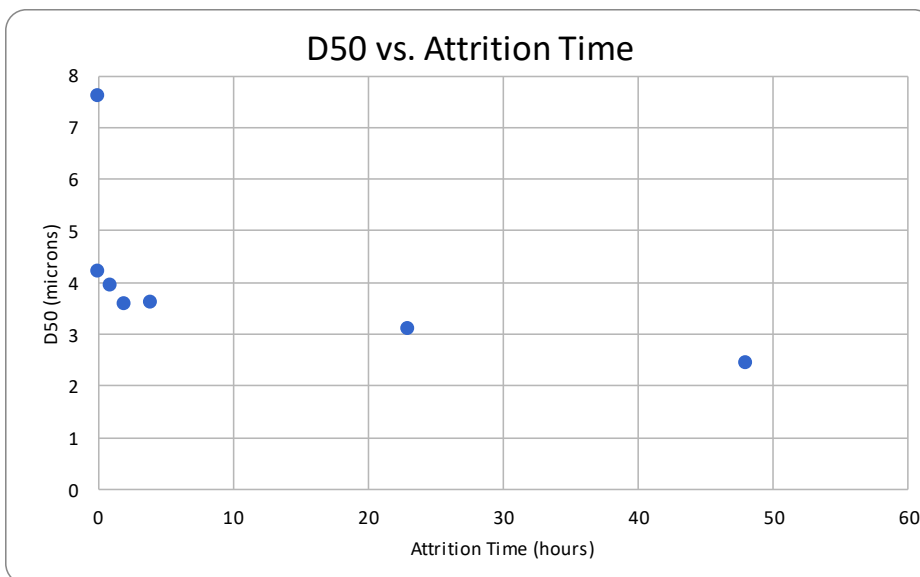


Figure 1: D50 of 19226 as a function of attrition time.

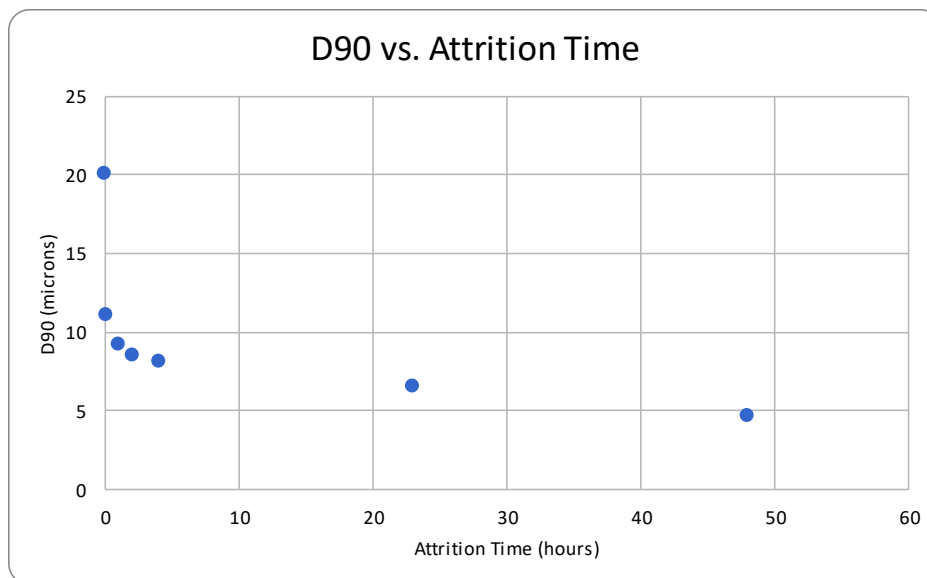


Figure 2: D90 of 19226 as a function of time.

The isopropanol was then driven off by heating on a hot plate, leaving the dried, milled ZnO tetrapods to be used in making inks.

5.2.3 Demonstration of diode using unmilled tetrapods

An “ink”, 19284, consisting of 99.0 grams of binder polymer and 1.0 gram of unmilled ZnO tetrapods was prepared by simple mixing on a magnetic stirrer. A Kapton film was used as a base and first treated with a corona to make it more ink receptive. A draw down of a silver nanoparticle ink, 18346-1Ag, was made on this Kapton film with a #3 bar to make the Schottky contact for the diode. After curing, the resulting silver layer had a mirror like appearance and a surface resistance of less than $1 \Omega/\square$. A #20 draw down bar was then used to place a thin layer of the ZnO tetrapod ink over the silver. This layer was then cured for 5 minutes at $\sim 540^\circ\text{F}$ ($\sim 282^\circ\text{C}$).

A Fluke 87III Multimeter in the diode setting was used as a check to determine if the device behaved as a diode. A copper bar was set on top of a portion of the silver layer that had not been overcoated with the ZnO tetrapod ink. Aluminum foil was then used as the ohmic contact above the zinc oxide layer, with a copper bar set on top of the foil. The meter read zero volts when the common electrode of the meter was connected to the copper bar on the silver and the positive lead on the bar on the aluminum foil. Then around 1.4-1.5 volts was measured when the leads were reversed, with the positive lead on the silver, as would be expected for a Schottky diode. Note that there were obvious streaks and imperfections in the ZnO layer from the draw down process. Areas could be found on the ZnO surface where the device would be “shorted” and the multimeter measurement in diode mode would give the same few hundred or so millivolt reading regardless of how the meter electrodes were configured.

To confirm this result, a second device was made in a similar manner to the first. A draw down of the silver ink created a thin, highly conductive silver layer. Then a #20 bar was used to make a layer of the 19284 ZnO tetrapod ink. Again, imperfections in the surface coating of the ZnO layer led to some places on the device “shorting”. But the device behaved as a Schottky diode with the aluminum foil with copper bar on top placed on several areas of the surface. This time, the voltage measured with the positive lead on the silver was higher, more in the range of 1.5-2.0 volts.

On this second device, a few areas were treated with a conductive carbon ink, T6, Batch 1, using a Q-tip like applicator to apply a small amount of ink to an area. The carbon ink was cured in the same way as the ZnO ink with a high temperature oven treatment. In several of these spots, the device behaved as a Schottky diode, but with a higher voltage ~2.5-3.0 volts. In some areas, treatment of with the carbon ink caused shorting, with roughly half a volt measured with either lead on the silver. In other areas of treatment with the carbon ink, possibly due to too little carbon being deposited, the device also did not work with an unmeasurable high voltage with either lead on the silver.

Table 2 below attempts a rough calculation of the thickness of the dried layer of tetrapods and cured binder polymer. Using the density of each component and the polymer solids content of the polymer solution, the table takes the ink recipe by weight and calculates a volume for each component. By volume, the ZnO tetrapods and polymer solids are only 12.3% of the volume of the ink. With the #20 bar laying down a nominal wet layer thickness of 50.8 microns, using this percentage gives a thickness of the solid layer of roughly 6.3 microns. This is just a rough approximation. It is to be expected that the tetrapods, with legs of 10 to 20 microns, would stand on the order of 17-35 microns above the surface. But since most of the volume of the solids is polymer, 6 microns should be a good approximation of the polymer layer thickness, with some legs of ZnO tetrapods sticking out above that surface.

Table 2: Parameters of ZnO tetrapod ink draw down layer.

Unmilled tetrapod fluid (19284) for draw down demonstration of diode					
Ingredient	% solids*	Density (g/cm³)	cm³/g	g	cm³
ZnO tetrapods	100	5.78	0.173	1.0	0.173
polymeric binder	100	1.2	0.833	14.1	11.75
water	0	1	1.000	84.9	84.9
				100.0	96.8
*solids that remain after curing					
Volume Fraction of Solids		12.3%			
Dry Layer Thickness, μ (#20 bar)		6.3			
Tetrapods by volume tetrapod in nonvolatile solids in draw down				1.5%	
Tetrapods by weight in nonvolatile solids in draw down				6.6%	

Note that by volume and by weight the unmilled tetrapods are only a small fraction of the dried ink layer. It apparently only takes this small amount of tetrapods to contact the aluminum foil or carbon ink layer and demonstrate diode-like behavior.

5.2.4 Attempts to construct diode using milled tetrapods

Using the simple recipe for the ZnO tetrapod “ink” that led to a working diode, a series of similar inks were made using the milled tetrapods. The milled tetrapods were expected to contain a few percent of ZnO as fragments that were on the order of 10 microns long. To make a working diode, these fragments would have to arrange themselves in a way that allowed contact with the silver surface below them and the aluminum or carbon layer above. While the fragments were long enough to do this in theory if they were oriented correctly, gravity would make the most likely orientation of these fragments as lying flat on the surface of the silver layer. The following series of “inks” shown in Table 3 were made, varying the proportion of milled tetrapods to polymer. None of them exhibited diode behavior.

5.2.5 Attempts to construct diode using a different geometry

Since the milled tetrapods were not expected to have the ability to orient in a vertical direction, the diode geometry described previously using layers stacked vertically was unlikely to work. It was decided to attempt a different geometry for the diode in which a Schottky contact was made by printing a silver ink and then an ohmic contact was printed adjacent to it using a carbon black ink. The key to this geometry is to keep the gap between the two contacts as small as possible to allow the milled tetrapods to span the gap when the ZnO ink was applied onto it. A gap of 10 microns or less was expected to be necessary to enable such a device.

Many attempts were made to print silver and carbon inks adjacent to each other leaving as small a gap as possible. Model inks containing milled and unmilled tetrapods and binding polymer were made and applied to the gaps but with no success in generating any kind of diode behavior. Several printers/fixtures were tried but none of them could lay down adjacent layers as required with a gap of 10 microns or less.

A paper by Chen et al.³ was found that described making gaps on the order of a micron by printing hydrophobic and hydrophilic inks adjacent to one another. The gap is set not by the motion quality of the printer but rather by the repulsion between the incompatible liquid layers.

This set in a motion an effort to design a carbon ink using a hydrophobic solvent. The hydrophilic ink was planned to be XACTIV’s existing silver nanoparticle ink. It was deemed easier to create a carbon ink in a hydrophobic solvent. Exxon’s Isopar solvents were considered initially but later work focused on toluene. Identifying appropriate dispersants for the carbon pigments in the new solvent proved very challenging as did identifying a suitable binding polymer. Several hydrophobic carbon/hydrophilic silver ink combinations were tried in various schemes to create gaps. For instance, one ink was

applied to a substrate with a draw down bar while the ink of opposite chemical character was deposited in a drop near the edge of the draw down. It soon became evident that the timing between application of the inks was a critical parameter as well as the amount of ink applied. Many experiments were performed using various ways to apply the inks and varying the time between applications and amounts applied. The resulting gaps created were observed under a microscope and, although some gaps appeared to be of the correct size, 10 microns or less, no diode was able to be created with either the milled or unmilled ZnO tetrapods.

The inks of opposite polarity used in the cited paper were then acquired from their respective suppliers and tried. The hydrophobic ink, UTDAglJ, was a 40% by weight silver ink acquired from UT Dots. The hydrophilic ink, Metalon JS-B40G, also was a 40% by weight silver ink acquired from Novacentrix. Many attempts were made to apply the hydrophobic UT Dots ink adjacent to XACTIV high conductivity aqueous carbon inks. Again, despite the gaps appearing to be the appropriate size of 10 microns or less, no diode was able to be demonstrated when the tetrapod fluids were applied across the gap and cured.

This was the state of the work when the project ended. Subsequently, XACTIV has acquired a Dimatix DMP-2381 printer like the one used in the paper by Chen et al. Should this work be continued, this would provide a better platform for applying the various inks.

Table 3: Parameters of ZnO milled tetrapod ink draw down layers.

Milled tetrapod fluid (19287-1) for draw down demonstration of diode					
Ingredient	% solids*	Density (g/cm³)	cm³/g	g	cm³
ZnO tetrapods	100	5.78	0.173	0.198	0.034
polymeric binder	100	1.2	0.833	2.813	2.345
water	0	1	1.000	16.930	16.930
				19.942	19.3
*solids that remain after curing					
Volume Fraction of Solids		12.3%			
		Wet	Dry		
Layer Thickness, μ (#10 bar)		25.4	3.1		
Layer Thickness, μ (#20 bar)		50.8	6.3		
Tetrapods by volume in nonvolatile solids in draw down				1.4%	
Tetrapods by weight in nonvolatile solids in draw down				6.6%	
Milled tetrapod fluid (19287-2) for draw down demonstration of diode					
Ingredient	% solids*	Density (g/cm³)	cm³/g	g	cm³
ZnO tetrapods	100	5.78	0.173	0.997	0.173
polymeric binder	100	1.2	0.833	2.707	2.256
water	0	1	1.000	16.291	16.291
				19.996	18.7
*solids that remain after curing					
Volume Fraction of Solids		13.0%			
		Wet	Dry		
Layer Thickness, μ (#10 bar)		25.4	3.3		
Layer Thickness, μ (#20 bar)		50.8	6.6		
Tetrapods by volume in nonvolatile solids in draw down				7.1%	
Tetrapods by weight in nonvolatile solids in draw down				26.9%	
Milled tetrapod fluid (19287-3) for draw down demonstration of diode					
Ingredient	% solids*	Density (g/cm³)	cm³/g	g	cm³
ZnO tetrapods	100	5.78	0.173	2.004	0.347
polymeric binder	100	1.2	0.833	2.565	2.138
water	0	1	1.000	15.438	15.438
				20.008	17.9
*solids that remain after curing					
Volume Fraction of Solids		13.9%			
		Wet	Dry		
Layer Thickness, μ (#10 bar)		25.4	3.5		
Layer Thickness, μ (#20 bar)		50.8	7.0		
Tetrapods by volume in nonvolatile solids in draw down				14.0%	
Tetrapods by weight in nonvolatile solids in draw down				43.9%	
Milled tetrapod fluid (19287-4) for draw down demonstration of diode					
Ingredient	% solids*	Density (g/cm³)	cm³/g	g	cm³
ZnO tetrapods	100	5.78	0.173	4.003	0.693
polymeric binder	100	1.2	0.833	2.280	1.900
water	0	1	1.000	13.719	13.719
				20.002	16.3
*solids that remain after curing					
Volume Fraction of Solids		15.9%			
		Wet	Dry		
Layer Thickness, μ (#10 bar)		25.4	4.0		
Layer Thickness, μ (#20 bar)		50.8	8.1		
Tetrapods by volume in nonvolatile solids in draw down				26.7%	
Tetrapods by weight in nonvolatile solids in draw down				63.7%	

5.3 References

5.3.1

1. Persson, E., “Printed Schottky Diodes base upon Zinc Oxide Materials”, Department of Science and Technology, Linköping University, SE-601 74 Norrköping, Sweden, 2013-12-18, LiU-ITN-TEK-A--13/073—SE
2. Pronin, I., Averin, I., Yakushova, N., Vishnevskaya, G., Sychov, M., Moshnikov, V., and Terukov, E., “Investigation of milling processes of semiconductor zinc oxide nanostructured powders by X-ray phase analysis”, *IOP Conference Series: Journal of Physics: Conference Series* **917** (2017) 032019 doi:10.1088/1742-6596/917/3/032019
3. Grubb, P., Subbaraman, H., Park, S., Akinwande, D., and Chen, R., “Inkjet Printing of High Performance Transistors with Micron order Chemically Set Gaps”, *Scientific Reports*, 2017, **7**, 1202.

5.3.2 Semiconductor Materials Reviews

4. Garlapati, S., Divya, M., Breitung, B., Kruk, R., Hahn, H., and Dasgupta, S., “Printed Electronics Based on Inorganic Semiconductors: From Processes and Materials to Devices”, *Advanced Materials*, 2018, **30**, 1707600.
5. Paterson, A. and Anthopoulos, T., “Enabling thin-film transistor technologies and the device metrics that matter”, *Nature Communications*, 2018, **9**, 5264.
6. Lu, B., Lan, H., and Liu, H., “Additive manufacturing frontier: 3D printing electronics”, *Opto-Electronic Advances*, 2018, **1**, 170004.
7. Semple, J., Georgiadou, D., Wyatt-Moon, G., Gelinck, G., Anthopoulos, T., “Flexible diodes for radio frequency electronics: a materials perspective”, *Semiconductor Science and Technology*, 2017, **32**, 123002.
8. Sun, Y. and Rogers, J., “Inorganic Semiconductors for Flexible Electronics”, *Advanced Materials*, 2007, **19**, 1897.

5.3.3 Silica/Silicon Films

9. Facchetti, A., "Printed diodes operating at mobile phone frequencies", *Proceedings of the National Academy of Sciences of the United States of America*, 2014, **111**,11917.
10. Sani, N., Robertsson, M., Cooper, P., Wang, X., Svensson, M., Ersman, P., Norberg, P., Nilsson, M., Nilsson, D, Liu, X., Hesselbom, H., Akesso, L., Fahlman, M., Crispin, X., Engquist, I., Berggren, M., and Gustafsson, G., "All-printed diode operating at 1.6 GHz", *Proceedings of the National Academy of Sciences of the United States of America*, 2014, **111**, 11943.
11. Harting, M., Zhang, J., Gamota, D., and Britton, D., "Fully printed silicon field effect transistors", *Applied Physics Letters*, 2009, **94**, 193509.
12. Lechner, R., Wiggers, H., Ebbers, A., Steiger, J., Brandt, M., and Stutzmann, M., "Thermoelectric effect in laser annealed printed nanocrystalline silicon layers", *Physica Status Solidi-Rapid Research Letters*, 2007, **1**, 262.
13. Ogawa, M., Kikuchi, T., "Preparation of Self-Standing Transparent Films of Silica-Surfactant Mesoporous Materials and the Conversion to Porous Silica Films", *Advanced Materials*, 1998, **10**, 1077.

5.3.4 Metal Oxide Thin Film Transistors

14. Bretos, I., Jimenez, R., Ricote, J., and Calzada, M., "Low-Temperature crystallization of solution-derived metal oxide thin films assisted by chemical processes", *Chemical Society Reviews*, 2018, **47**, 291.
15. Hu, H., Zhu, J., Chen, M., Guo, T., and Li, F., "Inkjet-printed p-type nickel oxide thin-film transistor", *Applied Surface Science*, 2018, **441**, 295.
16. Scheideler, W., Kumar, R., Zeumault, A., and Subramanian, V., "Low-Temperature-Processed Printed Metal Oxide Transistors Based on Pure Aqueous Inks", *Advanced Functional Materials*, 2017, **27**, 1606062.
17. Rho, Y., Kang, K-T., and Lee, D., "Highly crystalline Ni/NiO hybrid electrodes processed by inkjet printing and laser-induced reductive sintering under ambient conditions", *Nanoscale*, 2016, **8**, 8976.
18. Lee, J., Zhang, S., and Sun, S., "High-Temperature Solution-Phase Syntheses of Metal-Oxide Nanocrystals", *Chemistry of Materials*, 2013, **25**, 1293.
19. Jia, Q., McCleskey, T., Burrell, A., Lin, Y., Collis, G., Wang, H., and Li, A., "Polymer-assisted deposition of metal-oxide films", *Nature Materials*, 2004, **3**, 529.

5.3.5 ZnO Semiconductor

20. Zhang, Q., Xia, G., Li, L., Xia, W., Gong, H., and Wang, S., "High-performance Zinc-Tin-Oxide thin film transistors based on environment friendly solution process", *Current Applied Physics*, 2019, **19**, 174.
21. Mishra, Y. and Adelung, R., "ZnO tetrapod materials for functional applications", *Materials Today*, 2018, **21**, 631.
22. Al-Khanbashi, H., Shirbeeney, W., Al-Ghamdi, A., Bronstein, L., and Mahmoud, W., "Development of highly conductive and transparent copper doped zinc oxide thin films via 2-methoxyethanol modified sol-gel dip-coating technique", *Ceramics International*, 2014, **40**, 1927.
23. Ko, S., Lee, D., Hotz, N., Yeo, J., Hong, S., Nam, K., and Grigoropoulos, C., "Digital Selective Growth of ZnO Nanowire Arrays from Inkjet-Printed Nanoparticle Seeds on a Flexible Substrate", *Langmuir*, 2012, **28**, 4787.
24. Janotti, A. and Van de Walle, C., "Fundamentals of zinc oxide as a semiconductor", *Reports on Progress in Physics*, 2009, **72**, 126501.

5.3.6 Chitosan Dielectric

25. Liang, J., Wang, J., Li, S., Xu, L., Wang, R., Chen, R., and Sun, Y., "The size-controllable preparation of chitosan/silver nanoparticle composite microsphere and its antimicrobial performance", *Carbohydrate Polymers*, 2019, **220**, 22.
26. Singh, R., Lin, Y-T., and Ko, F-H., "Aqueous Solution-Processable, Flexible Thin-Film Transistors Based on Crosslinked Chitosan Dielectric Thin Films", *Macromolecular Materials and Engineering*, 2018, **303**, 1700468.